國 立 交 通 大 學

電信工程學系碩士班
碩士論文

適用於時變正交分頻多工系統之干擾消除技術

Interference Cancellation in OFDM Systems over

Time-Varying Channels

研 究 生：蔡宗翰　　　　　Student: Tsung-Han Tsai

指導教授：李大嵩 博士　　Advisor: Dr. Ta-Sung Lee

中 華 民 國 九 十 五 年 六 月

適用於時變正交分頻多工系統之干擾消除技術

Interference Cancellation in OFDM Systems over Time-Varying Channels

研 究 生：蔡宗翰　　　　　　　Student: Tsung-Han Tsai

指導教授：李大嵩 博士　　　　　Advisor: Dr. Ta-Sung Lee

國立交通大學

電信工程學系碩士班

碩士論文

A Thesis
Submitted to Institute of Communication Engineering
College of Electrical Engineering and Computer Science
National Chiao Tung University
in Partial Fulfillment of the Requirements
for the Degree of
Master of Science
in
Communication Engineering
June 2006
Hsinchu, Taiwan, Republic of China

中 華 民 國 九 十 五 年 六 月

適用於時變正交分頻多工系統之干擾消除技術

學生：蔡宗翰　　　　　　　　　　指導教授：李大嵩 博士

國立交通大學電信工程學系碩士班

摘要

　　正交分頻多工系統為新一代無線通訊系統最常使用的技術，如 IEEE 802.11a/g/n、 IEEE 802.16、IEEE 802.20、數位電視、數位廣播等許多系統均採用此技術。傳統的正交分頻多工系統並不適用在高速移動的環境中，然而移動傳輸是未來無線通訊系統的趨勢之一，如 IEEE 802.16e 可支援到車速 120 km/hour，而 IEEE 802.20 更可支援到車速 250 km/hour。傳統的正交分頻多工系統可以有效率地使用在非時變通道中，且僅需簡單的等化器，即可修正通道效應，但在移動的環境中，通道隨著時間改變，使得接收端的子載波失去正交性，因而導致子載波之間的相互干擾，使得解調變後的效能降低。雖然最小均方差等化器可以改善此種干擾問題，然而其複雜度過高，不利於正交分頻多工系統採用。在本論文中，吾人利用移動傳輸通道的特性對共軛梯度法做最佳事先處理，來降低最小均方差等化器所需反矩陣運算的複雜度，使得接收端得以有效消去子載波間的干擾，而能在移動的環境下運作。吾人藉由電腦模擬驗證此一新等化器在移動的環境中，可有效改善位元錯誤率。

Interference Cancellation in OFDM Systems over Time-Varying Channels

Student: Tsung-Han Tsai   Advisor: Dr. Ta-Sung Lee

Institute of Communication Engineering

National Chiao Tung University

Abstract

Orthogonal Frequency Division Multiplexing (OFDM) is a popular technique in modern wireless communications. There are many systems adopting the OFDM technique, such as IEEE 802.11 a/g/n, IEEE 802.16, IEEE 802.20, Digital Video Broadcasting, Digital Audio Broadcasting, etc. On the other hand, mobile transmission is a trend in future wireless communications. For example, IEEE 802.16e supports vehicle speed up to 120 km/hour, and IEEE 802.20 supports vehicle speed up to 250 km/hour. OFDM systems can be used efficiently in time invariant environments with one-tap equalizers. However, subcarriers are no longer orthogonal to each other in time-varying channels, and this causes the intercarrier interference (ICI) and degrades the system performance. Although the minimum mean square error (MMSE) equalizer can be employed to solve this problem, it requires a high complexity and is impractical for an OFDM receiver to be implemented. To alleviate this problem, we propose a conjugate gradient based method with optimal precondition by employing the property of the mobile channel, which can reduce the complexity of the matrix inversion problem in the MMSE equalizer. Finally, we evaluate the performance of the proposed system and confirm that it achieves good BER performance in mobile environments.

Acknowledgement

I would like to express my deepest gratitude to my advisor, Dr. Ta-Sung Lee, for his enthusiastic guidance and great patience. I learn a lot from his positive attitude in many areas. Heartfelt thanks are also offered to all members in the Communication System Design and Signal Processing (CSDSP) Lab for their constant encouragement. Finally, I would like to show my sincere thanks to my parents for their invaluable love.

Contents

List of Figures

List of Tables

Acronym Glossary

ADC   analog-to-digital conversion

CP   cyclic prefix

CG   Conjugate gradient

DFT   discrete Fourier transform

DIOM   direct incomplete orthogonalization method

FFT   Fast Fourier Transform

FIR   finite impulse response

FSK   frequency shift keying

ICI   intercarrier interference

IOM   incomplete orthogonal method

ISI   intersymbol interference

IFFT   Inverse Fast Fourier Transform

LS   least square

LANs   local-area networks

MCM   multicarrier modulation

MMSE   minimum mean-square error

NLOS   non-LOS

OFDM   orthogonal frequency division multiplexing

PAPR   peak-to-average power ratio

PCG   preconditioned conjugate gradient

PHY   Physical Layer

PSD   power spectral density

QPSK   quadrature phase shift keying

RF   radio frequency

SIR   signal-to-interference ratio

SNR   signal-to-noise ratio

Notations

F	DFT matrix
h	time domain channel tap
H	time domain channel matrix
A	frequency domain channel matrix
N_c	number of subcarriers
N_{cp}	number of guard interval samples
N_{DT}	number of data tones
M	modulation order
η	AWGN noise
s	transmitted frequency domain signal
x	transmitted time domain signal
y	received signal after DFT
R	information data rate
L	channel order
T_s	symbol duration
W	equalizer weights
σ_n^2	noise power
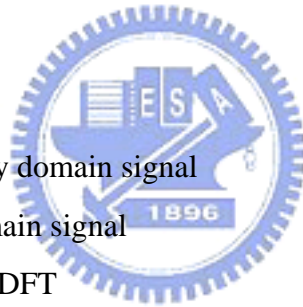
Chapter 1

Introduction

Orthogonal Frequency Division Multiplexing (OFDM) is a popular technique in modern wireless communication systems. There are many systems adopting this technique, such as IEEE 802.11 a/g/n, IEEE 802.16, IEEE802.20, Digital Video Broadcasting, Digital Audio Broadcasting, etc. In an OFDM system, the bandwidth is divided into several orthogonal subchannels for transmission. A cyclic prefix (CP) is inserted before each symbol. Therefore, if the delay spread of the channel is shorter than the length of the cyclic prefix, the intercarrier symbol interference (ISI) can be eliminated due to the cyclic prefix. On the other hand, subcarriers in OFDM are orthogonal to each other over time-invariant channels, so the conventional OFDM system only requires one-tap equalizers to compensate the channel response. This characteristic simplifies the design of the OFDM receiver, for this reason, the OFDM technique is widely used in wireless communication systems.

The mobile transmission is a trend in future wireless communications. Many systems support the mobile transmission, such as IEEE 802.16e, IEEE 802.20, DVB-H. and these systems also adopt the OFDM technique. However, while OFDM system is applied in mobile environments, the variation of channels destroys the orthogonality among subcarriers and therefore the intercarrier interference (ICI) arises. The conventional one-tap equalizer is insufficient for the mobile OFDM system because

the ICI degrades the system performance; the ICI cancellation technique plays an important role in mobile OFDM systems.

Many methods for ICI cancellation have been proposed. By mapping the data into groups of subcarriers, intercarrier interference self-cancellation scheme [1], [2] has been proposed. This scheme can reduce the computation complexity while sacrificing the transmission bandwidth efficiency. An error bound of the mobile OFDM system and an MMSE-SIC (minimum mean square error-successive interference cancellation) equalizer for canceling ICI are proposed [3]. Alternatively, an MMSE-PIC (parallel interference cancellation) equalizer is proposed in [4]. However, the computation complexity of these schemes is proportional to the square of the FFT size. On the other hand, some low complexity equalizers whose computation complexity increases linearly with the FFT size have been proposed in [5], [6], [7]. Those equalizers are based on approximations of the mobile channels. The ICI cancellation scheme in [5] can only be used in slow time-varying channel because of the rough approximation. An MMSE equalizer with a modified channel approximation and time-domain windowing technique for enhancing this approximation are introduced [6]. Another simple MMSE equalizer with the same channel approximation in [6] has been proposed [7] based on the LDL$^{\text{H}}$ factorization.

This paper proposes a low-complexity MMSE equalizer based on the band channel approximation in [6] and a conjugate gradient based method with optimal preconditioning by employing the property of the mobile channel, which can reduce the complexity of the matrix inversion problem in the MMSE equalizer. The preconditioned conjugate gradient (PCG) algorithm is one of the best known Krylov subspace method for solving spare, positive definite systems of equations which is equivalent to the matrix inversion problem in the MMSE equalizer. Many kinds of

Krylov subspace methods are introduced in [8], [9], [10]. The iterative programs for simulations in this thesis are based on the template book [11].

This thesis is organized as follows. In Chapter 2, the general idea of the OFDM system and the challenges it is faced with mobile environments are described. In Chapter 3, the basic idea of the Krylov subspace methods and the conjugate gradient (CG) methods are introduced. In Chapter 4, the proposed interference cancellation scheme is presented and analyzed. We evaluate the performance of the proposed system and confirm that it achieves good BER performance in mobile environments. In Chapter 5, we conclude this thesis and propose some potential future works.

Chapter 2

Overview of Orthogonal Frequency Division Multiplexing (OFDM) Systems

In this chapter, an overview of OFDM systems will be given in Section 2.1. OFDM is an efficient technique for high data rate transmission such as IEEE 802.11 a/g/n, IEEE 802.16. We will show the advantage of OFDM system and why traditional OFDM system can be efficient in frequency-selective environments. Furthermore, the challenge of OFDM system in mobile environments is presented in Section 2.2 and some existing techniques for mobile OFDM system is introduced in Section 2.3

2.1 Orthogonal Frequency Division Modulation Systems

OFDM is a special case of multicarrier transmission, where a single data stream is transmitted over a number of low data rate subcarriers. OFDM can be thought of as a hybrid of multicarrier modulation (MCM) and frequency shift keying (FSK) modulation scheme. The principle of MCM is to transmit data by dividing the data stream into several parallel data streams and modulate each of these data streams onto

individual subcarriers. FSK modulation is a technique whereby data is transmitted on one subcarrier from a set of orthogonal subcarriers in symbol duration. Orthogonality between these subcarriers is achieved by separating these subcarriers by an integer multiples of the inverse of symbol duration of the parallel data streams. With the OFDM technique used, all orthogonal subcarriers are transmitted simultaneously. In other words, the entire allocated channel is occupied through the aggregated sum of the narrow orthogonal subbands.

The main reason to use OFDM systems is to increase the robustness against frequency-selective fading or narrowband interference. In a single carrier system, a single fade or interference can cause the entire link fail, but in a multicarrier system, only a small amount of subcarriers will be affected. Then the error correction coding techniques can be used to correct errors. The equivalent complex baseband OFDM signal can be expressed as

$$x(t) = \begin{cases} \displaystyle\sum_{k=-\frac{N_c}{2}}^{\frac{N_c}{2}-1} d_k \phi_k(t) & 0 \le t \le T \\ 0 & \text{Otherwise} \end{cases} = \left[\sum_{k=-\frac{N_c}{2}}^{\frac{N_c}{2}-1} d_k \phi_k(t) \right] u_T(t) \tag{2.1}$$

where N_c is the number of subcarriers, T is the symbol duration, d_k is the transmitted subsymbol (M-PSK or M-QAM), $\phi_k(t) = e^{j2\pi f_k t}/\sqrt{T}$ is the kth subcarrier with the frequency $f_k = k/T$, and $u_T(t)$ is the time windowing function. Using the correlator-based OFDM demodulator, the output of the jth branch can be presented as

$$y_j = \int_0^T x(t)\phi_j^*(t)dt = \frac{1}{T} \sum_{k=-\frac{N_c}{2}}^{\frac{N_c}{2}-1} d_k \int_0^T e^{j2\pi\frac{k-j}{T}t} dt \tag{2.2}$$

$$= d_j$$

By sampling $x(t)$ with the sampling period $T_d = T/N_c$, the discrete time signal x_n can be expressed as

$$x_n = x(t)\big|_{t=nT_d} = \begin{cases} \dfrac{1}{\sqrt{N_c}} \displaystyle\sum_{k=-\frac{N_c}{2}}^{\frac{N_c}{2}-1} d_k e^{j2\pi\frac{k}{N_c}n} \ , & 0 \le n \le N_c - 1 \\ 0 & , \quad \text{Otherwise} \end{cases} = \text{IFFT}\{d_k\} \qquad (2.3)$$

Note that x_n is the Inverse Fast Fourier Transform (IFFT) output of the N input data subsymbols. Similarly, the output of the j-th branch can also be presented in the digital form

$$y_j = \text{FFT}\{x_n\} = \frac{1}{\sqrt{N_c}} \sum_{n=0}^{N_c-1} x_k e^{-j2\pi\frac{j}{N_c}n} = \sum_{k=-\frac{N_c}{2}}^{\frac{N_c}{2}-1} x_k \delta[k-j] = d_j \qquad (2.4)$$

In theory, the orthogonality of subcarriers in OFDM systems can be maintained and individual subcarriers can be completely separated by the Fast Fourier Transform (FFT) at the receiver when there are no intersymbol interference (ISI) and intercarrier interference (ICI) introduced by transmission channel distortions. However, it is impossible to obtain these conditions in practice. In order to eliminate ISI completely, a guard interval is imposed into each OFDM symbol. The guard interval is chosen larger than the expected delay spread, such that the multipath from one symbol cannot interfere with the next symbol. The guard interval can consist of no signals at all. However, the effect of ICI would arise in that case due to the loss of orthogonality between subcarriers. To eliminate ICI, the OFDM symbol is cyclically extended in the guard interval to introduce cyclic prefix (CP) as shown in Figures 2.1 and 2.2. This ensures that delayed replicas of the OFDM symbol always have an integer number of cycles within the FFT interval, as long as the delay is smaller than the guard interval.

| $X_{N-N_{cp}}$ | | | X_{N-1} | X_0 | X_1 | | X_{N-1} |

Cyclic Prefix ⟶ ⟵   Useful Part ⟶

N_{cp} N

⟵ Complete OFDM Signal ⟶

$N+N_{cp}$
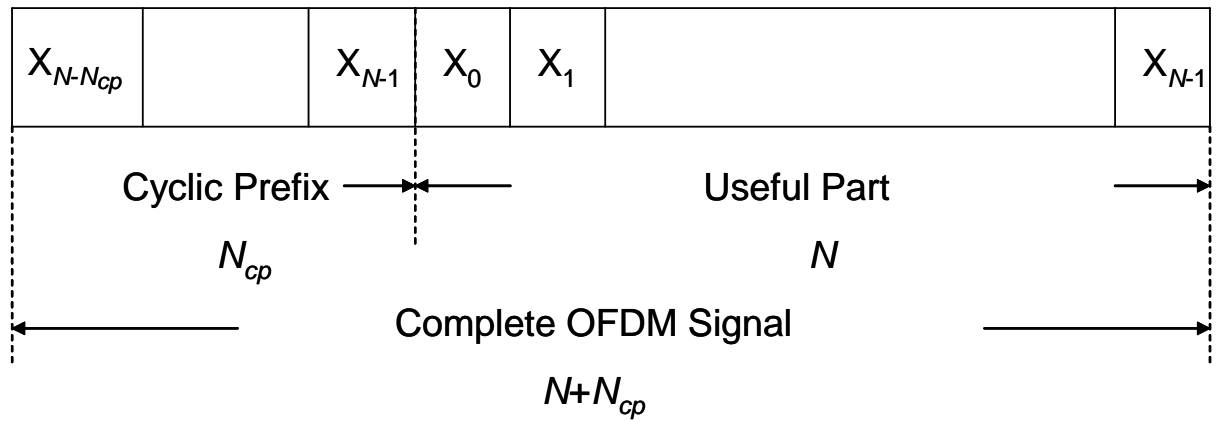
Figure 2.1: OFDM signal with cyclic prefix extension.
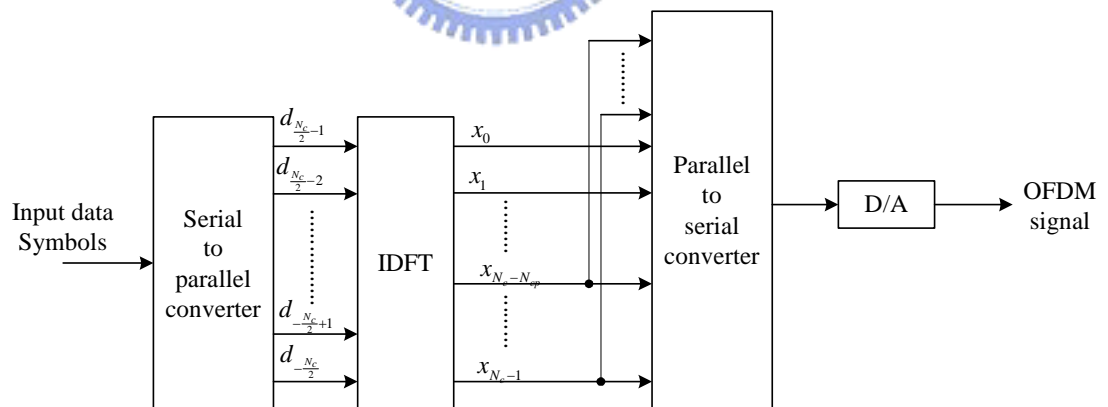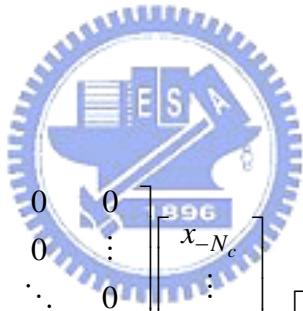
Figure2.2: A digital implementation of appending cyclic prefix into the OFDM signal in the transmitter.

As a result, the delayed multipath signals which are smaller than the guard interval will not cause ICI. The complete OFDM signal with CP is given by

$$
\tilde{x}_n = \begin{cases} \dfrac{1}{\sqrt{N_c}} \displaystyle\sum_{k=-\frac{N_c}{2}}^{\frac{N_c}{2}-1} d_k e^{j2\pi\frac{k}{N_c}(n-N_{cp})} & 0 \le n \le N_c + N_{cp} - 1 \\[2ex] 0 & \text{Otherwise} \end{cases}
\tag{2.5}
$$

where N_{cp} is the number of samples in CP. Due to CP, the transmitted OFDM symbol becomes periodic, and the linear convolution process of the transmitted OFDM symbols with the channel impulse responses will become a circular convolution one. Assuming the value of N_{cp} is larger than the channel length, the received signal vector can be expressed as

$$
\mathbf{y} = \mathbf{H}\mathbf{x} + \boldsymbol{\eta}
$$

$$
\underbrace{\begin{bmatrix} y_0 \\ \vdots \\ y_{N_c-1} \end{bmatrix}}_{\mathbf{y}} = \underbrace{\begin{bmatrix} h_0 & 0 & 0 & 0 \\ h_1 & h_0 & 0 & \vdots \\ \vdots & h_1 & \ddots & 0 \\ h_{N_{cp}} & \vdots & \ddots & h_0 \\ 0 & h_{N_{cp}} & \vdots & h_1 \\ \vdots & 0 & \ddots & \vdots \\ 0 & \cdots & 0 & h_{N_{cp}} \end{bmatrix}}_{\mathbf{H}} \underbrace{\begin{bmatrix} x_{-N_c} \\ \vdots \\ x_{-1} \\ x_0 \\ \vdots \\ x_{N_{cp}-1} \end{bmatrix}}_{\mathbf{x}} + \underbrace{\begin{bmatrix} \eta_0 \\ \vdots \\ \eta_{N_c-1} \end{bmatrix}}_{\boldsymbol{\eta}}
\tag{2.6}
$$

Applying SVD on the channel response, we have

$$
\mathbf{H} = \mathbf{U}\boldsymbol{\Sigma}\mathbf{V}^H
\tag{2.7}
$$

where $\mathbf{U}$ and $\mathbf{V}$ are unitary matrices, and $\boldsymbol{\Sigma}$ is a diagonal matrix. Substituting Equation (2.7) and the equalities of $\mathbf{x} = \mathbf{V}\mathbf{X}$ and $\mathbf{Y} = \mathbf{U}^H\mathbf{y}$ into Equation (2.6), the received signal vector can be written as

$$\mathbf{Y} = \mathbf{U}^H \mathbf{y} = \mathbf{U}^H(\mathbf{H}\mathbf{x} + \boldsymbol{\eta}) = \mathbf{U}^H \mathbf{H}\mathbf{V}\mathbf{X} + \underbrace{\mathbf{N}}_{\mathbf{U}^H \boldsymbol{\eta}} = \boldsymbol{\Sigma}\mathbf{X} + \mathbf{N} \tag{2.8}$$

This means that the output $\mathbf{Y}$ can be expressed in terms of the product of $\boldsymbol{\Sigma}$ and $\mathbf{X}$ plus noise. When $x_{-i} = x_{N-i}$ for $i = 1, \dots, N_{cp}$, a more compact matrix form of the guard interval can be written as

$$
\begin{bmatrix} y_0 \\ \vdots \\ y_{N_c-1} \end{bmatrix} =
\begin{bmatrix}
h_0 & 0 & \cdots & 0 & h_{N_{cp}} & \cdots & h_1 \\
h_1 & h_0 & \ddots & \cdots & 0 & \ddots & \vdots \\
\vdots & h_1 & \ddots & \ddots & \ddots & \ddots & h_{N_{cp}} \\
h_{N_{cp}} & \vdots & \ddots & h_0 & 0 & \cdots & 0 \\
0 & h_{N_{cp}} & \ddots & h_1 & h_0 & \cdots & \vdots \\
\vdots & \ddots & \ddots & \ddots & \ddots & \ddots & 0 \\
0 & 0 & \cdots & h_{N_{cp}} & h_{N_{cp}-1} & \cdots & h_0
\end{bmatrix}
\begin{bmatrix} x_0 \\ \vdots \\ x_{N_c-1} \end{bmatrix} +
\begin{bmatrix} \eta_0 \\ \vdots \\ \eta_{N_c-1} \end{bmatrix} \tag{2.9}
$$

where $\mathbf{H}$ becomes a circulant matrix ($\mathbf{H} = \mathbf{F}^H \boldsymbol{\Lambda} \mathbf{F}$) and $\mathbf{Q}$ is a discrete Fourier transform (DFT) matrix with the lth entry as

$$\mathbf{F}_l = \frac{1}{\sqrt{N_c}} e^{-j2\pi \frac{l}{N_c}} \tag{2.10}$$

As in Equation (2.8), the received signal $\mathbf{y}$ can be transformed into $\mathbf{Y}$

$$\mathbf{Y} = \mathbf{F}^H \mathbf{y} = \mathbf{F}^H(\mathbf{H}\mathbf{x} + \boldsymbol{\eta}) = \underbrace{\mathbf{F}^H \mathbf{H} \mathbf{F}^H}_{\boldsymbol{\Sigma}} \mathbf{X} + \underbrace{\mathbf{F}^H \boldsymbol{\eta}}_{\mathbf{N}}$$
$$= \boldsymbol{\Sigma}\mathbf{X} + \mathbf{N} \tag{2.11}$$

According to Equation (2.11), by adding CP to the OFDM symbol, the modulation in OFDM is equivalent to multiplying the frequency domain signals of the OFDM symbol with the channel's frequency response $\boldsymbol{\Sigma}$.

The block diagrams of the OFDM transceiver is shown in Figure 2.3, where the upper path is the transmitter chain and lower path corresponds to the receiver chain. In the center, IFFT modulates a block of input values onto a number of subcarriers. In the

receiver, the subcarriers are demodulated by the FFT, which performs the reverse operation of the IFFT. In fact, the IFFT can be made using the FFT by conjugating input and output of the FFT and dividing the output by the FFT size. This makes it possible to use the same hardware for both transmitter and receiver. This complexity saving is only possible when the transceiver doesn't have to transmit and receive simultaneously. The functions before the IFFT can be discussed as follows. Binary input data is first encoded by a forward error correction code. The encoded data is then interleaved and mapped onto QAM values. In the receiver path, after passing the radio frequency (RF) part and the analog-to-digital conversion (ADC), the digital signal processing starts with a training sequence to determine symbol timing and frequency offset. The FFT is used to demodulate all subcarriers. The FFT outputs are mapped onto binary values and decoded to produce binary output data. In order to successfully map the QAM values onto binary values, the reference phases and amplitudes of all subcarriers have to be acquired first.
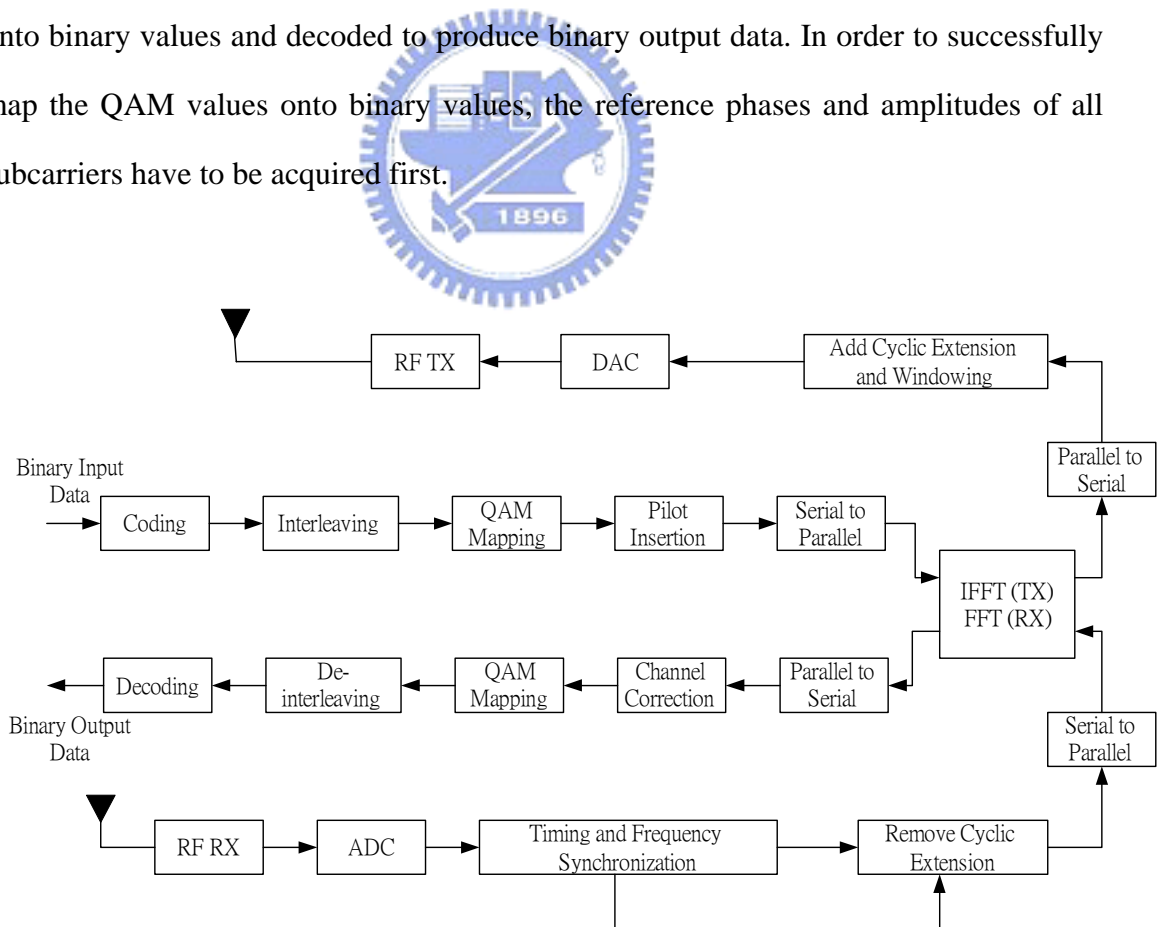
Figure2.3: Black diagrams of the OFDM transceiver.

In conclusion, OFDM is a powerful modulation technique that simplifies the removal of distortion due to the multipath channel and increases bandwidth efficiency. The key advantages of OFDM transmission scheme can be summarized as follows:

1. OFDM is an efficient way to deal with multipath. For a given delay spread, the implementation complexity is significantly lower than that of a single carrier system with an equalizer.

2. In relative slow time-varying channels, it is possible to significantly enhance the capacity by adapting the data rate per subcarrier according to the signal-to-noise ratio (SNR) of that particular subcarrier.

3. OFDM is robust against narrowband interference because such interference affects only a small amount of subcarriers.

4. OFDM makes single-frequency networks possible, which is especially attractive for broadcasting applications.
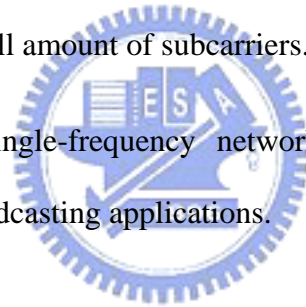
2.2 Challenges to Orthogonal Frequency Division Modulation Systems in Mobile Environments

The most important issue of the OFDM technique in time varying channels is that the ICI degrades the system performance. In this section, we will first introduce the mobile OFDM system model, and then discuss why the ICI is produced.

2.2.1 OFDM System Model over Time-Varying Channels

The OFDM system model over time-varying channels is considered here. Assuming that $\mathbf{s}^{(i)} = [s_0^i, \ldots s_{N-1}^{(i)}]^T$ is the i-th "frequency-domain" symbols, the OFDM symbol can be converted to "time-domain" symbols by N-point IDFT operation as

$$x^{(i)}(n) = \frac{1}{\sqrt{N}} \sum_{k=0}^{N-1} s_k^{(i)} e^{j\frac{2\pi}{N}kn}, \quad -N_c \leq n < N \tag{2.12}$$

where $x(n)$ is serially transmitted over noisy time-varying multipath channels, incorporates a cyclic prefix of length N_c. The channel is modeled by the time-varying discrete impulse response, $h(n,l)$, which is defined as the response of time n to an impulse response applied at time n-l.

The received sample sequence which is the convolution between the transmitted symbol and the time-varying channels can be written as

$$r^{(i)}(n) = \sum_{l=0}^{v-1} h^{(i)}(n,l) x^{(i)}{}_{n-l} + \eta_n^{(i)}, \quad 0 \leq n < N \tag{2.13}$$

where v is the maximum delay spread of the channel, N_c is the length of CP, and z_n are the samples of additive white Gaussian noise (AWGN), with variance σ^2. For the ISI free case, the delay spread of the channel should be shorter than the length of CP, as follows $v \leq N_c$.

Then the receiver computes an N-point DFT operation to obtain the frequency-domain signal

$$y^{(i)}(m) = \frac{1}{\sqrt{N}} \sum_{n=0}^{N-1} r_n^{(i)} e^{j\frac{2\pi}{N}mn}, \quad -N_c \leq n < N \tag{2.14}$$

Let $\mathbf{F}(l,k) = \frac{1}{\sqrt{N}} e^{-j(2\pi/N)lk}$, $0 \le l, k \le N\text{-}1$ be the standard N-dimensional DFT

matrix, Equation (2.12) can be written in matrix form

$$
\begin{bmatrix} r_0^{(i)} \\ \vdots \\ r_{N-1}^{(i)} \end{bmatrix} = \begin{bmatrix} h^{(i)}(0,0) & 0 & \cdots & h^{(i)}(0,L-1) & \cdots & h^{(i)}(0,1) \\ h^{(i)}(1,1) & h^{(i)}(1,0) & \ddots & 0 & \ddots & \vdots \\ \vdots & h^{(i)}(2,1) & \ddots & \ddots & 0 & h^{(i)}(L-2,L-1) \\ h^{(i)}(L-1,L-1) & \vdots & \ddots & 0 & \vdots & 0 \\ 0 & h^{(i)}(L,L-1) & \ddots & h^{(i)}(N+L-1,0) & 0 & \vdots \\ \vdots & \ddots & \ddots & \vdots & & 0 \\ 0 & 0 & \cdots & h^{(i)}(N-1,L-2) & & h^{(i)}(N-1,0) \end{bmatrix} \begin{bmatrix} x_0^{(i)} \\ \vdots \\ x_{N-1}^{(i)} \end{bmatrix} + \begin{bmatrix} \eta_0^{(i)} \\ \vdots \\ \eta_{N-1}^{(i)} \end{bmatrix}
$$

$$(2.15)$$

$h^{(i)}(n,l)$ represents the channel response of the l th tap at the time instance n, we can

rewrite the above equation in matrix form as

$$
\mathbf{r}^{(i)} = \mathbf{H}^{(i)}\mathbf{x}^{(i)} + \mathbf{\eta}^{(i)}, \quad 0 \le n < N \tag{2.16}
$$

where $\mathbf{r}^{(i)} = [r_0^{(i)}, \ldots, r_{N-1}^{(i)}]^T$, $\mathbf{\eta}^{(i)} = [\eta_0^{(i)}, \ldots, \eta_{N-1}^{(i)}]^T$, and $\mathbf{x}^{(i)} = [x_0^{(i)}, \ldots, x_{N-1}^{(i)}]^T$, $\mathbf{H}$ is

the time-varying channel matrix. Equation (2.16) can be rewritten as

$$
\begin{aligned} \mathbf{r}^{(i)} &= \mathbf{H}^{(i)}\mathbf{x}^{(i)} + \mathbf{\eta}^{(i)} \\ &= \mathbf{H}^{(i)}\mathbf{F}^H\mathbf{s}^{(i)} + \mathbf{\eta}^{(i)} \end{aligned} \tag{2.17}
$$

We define $\mathbf{A^{(i)}} = \mathbf{F}\mathbf{H}^{(i)}\mathbf{F}^H$ as the frequency domain channel matrix and Equation (2.14)

can be rewritten in vector form as

$$
\begin{aligned} \mathbf{y}^{(i)} &= \mathbf{F}\mathbf{r}^{(i)} = \mathbf{F}\mathbf{H}^{(i)}\mathbf{x}^{(i)} + \mathbf{F}\mathbf{\eta}^{(i)} \\ &= \mathbf{F}\mathbf{H}^{(i)}\mathbf{F}^H\mathbf{s}^{(i)} + \mathbf{F}\mathbf{\eta}^{(i)} = \mathbf{A}^{(i)}\mathbf{s}^{(i)} + \mathbf{z}^{(i)} \end{aligned} \tag{2.18}
$$

where $\mathbf{A^{(i)}}$ has the form

$$
\mathbf{A}^{(i)} = \begin{bmatrix} A(0,0) & \cdots & A(0,N-1) \\ \vdots & \ddots & \vdots \\ A(N-1,0) & \cdots & A(N-1,N-1) \end{bmatrix} \tag{2.19}
$$

which is called "equivalent frequency domain channel", and the non-diagonal terms of **A** produce the ICI.

2.2.2 Intercarrier Interference in OFDM System due to Time-Varying Channels

In time-invariant channels, the **A** matrix in Equation (2.19) will be a diagonal matrix, so the conventional OFDM systems can compensate the fading channel with one-tap equalizers. In time-varying channel, the **A** matrix is no longer a diagonal matrix, so it will have a poor performance if one-tap equalizers are used. It can be indicated that the non-diagonal terms in the **A** matrix are the ICI terms.

We analyze the ICI power based on the theorem in [5], [6]. Assuming a typical wide-sense stationary uncorrelated scattering (WSSUS) channel model [12] as below

$$E\{h(n,l)h^*(n-q,l-m)\} = r_t(q)\sigma_l^2\delta(m)$$

where $r_t(q)$ is the normalized tap autocorrelation, and σ_l^2 is the variance of the lth tap.

Since the non-diagonal terms in the **A** matrix are the intercarrier interference terms, we will compute the power of these non-diagonal terms. Let $A(n,l)$ be the n-th row, l-th column term of **A**, and $u(n)$ denotes the N-point rectangular window. Finally, we obtain

$$E\left\{|h(c,d)|^2\right\} = \frac{1}{N^2}\sum_{n,l,m,p} u(n)u(m)E\left\{h(n,l)h^*(m,p)\right\} \times \exp\left(\frac{j2\pi}{N}\left(pk - lk + md - nd\right)\right)$$

$$= \frac{1}{N^2}\sum_{l=-\infty}^{\infty}\sigma_l^2\sum_{n,m=-\infty}^{\infty} u(m)u(n)r_t(n-m)\exp(\frac{j2\pi}{N}(md-nd))$$

$$= \frac{1}{N^2} \sum_{l=-\infty}^{\infty} \sigma_l^2 \sum_{p=-\infty}^{\infty} \sum_{n=-\infty}^{\infty} u(m)u(n)r_t(q)\exp(^{-j2\pi pc}\!/_N) \qquad (2.20)$$

where $h(\pm n,:)$ denotes the nth supper or upper-diagonal. Assuming Rayleigh fading as in [10], we obtain

$$r_t(q) = J_0(2\pi f_d T_s q)$$

$$S(\phi) = \begin{cases} \dfrac{1}{\sqrt{(2\pi f_d T_s)^2 - \phi^2}} &, \ |\phi| \le 2\pi f_d T_s \\ 0 &, \quad \text{otherwise} \end{cases} \qquad (2.21)$$

where J_0 denotes the first kind zeroth-order Bessel function, and $f_d T_s$ is the maximum Doppler shift normalized to OFDM symbol rate.
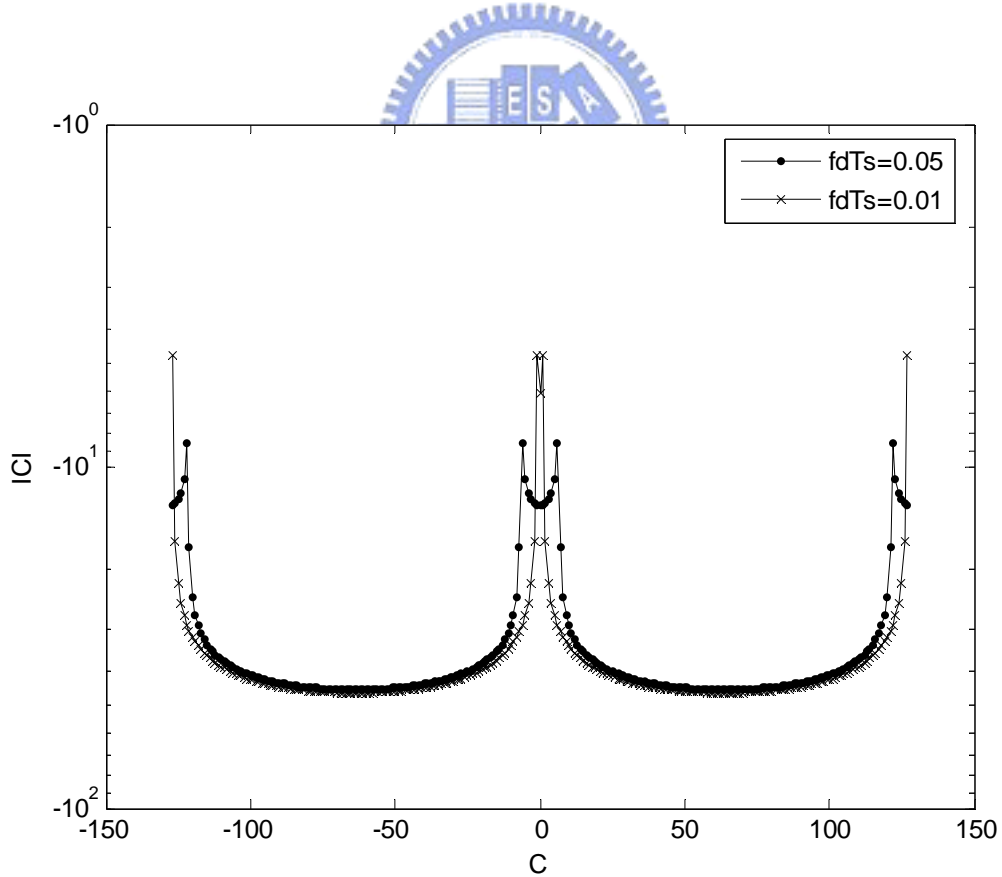

Figure2.4: ICI variance versus c (c is the index of super- or sub- diagonal)

By Equations (2.20) and (2.21), we can simulate the power of the non-diagonal terms, which is the terms caused the ICI. Figure.2.4 shows the computer simulations according to Equations (2.20) and (2.21). We can observe that the coefficients of the frequency domain channel matrix have most power on the central band and the edges of the channel matrix. One kind of channel approximation based on this property is described in Chapter 4. This channel approximation is the base of the low-complexity algorithm which will be described later.

2.3 Existing Techniques for OFDM Systems over Time-Varying Channels

OFDM is a strong candidate for high-data-rate systems over wireless channels. High data rates give rise to frequency-selective channels, while mobility and frequency errors introduce time-selective channel. Due to the analysis in Section 2.2, we show that the traditional OFDM system is sensitive to time-varying channels. Some techniques have been proposed to mitigate the ICI. We will first introduce ICI self-cancellation scheme [1], [2], which is originally used in compensating frequency errors and also valid over time-varying channels. Then we will show the frequency domain equalizer technique for compensating the ICI.

2.3.1 Intercarrier Interference Self-Cancellation Scheme

This method is proposed in [1], [2]. The ICI self-cancellation scheme is a simple way for suppressing ICI in OFDM system. It is to modulate one data symbol onto adjacent pairs of subcarriers rather than onto single subcarriers. By this way, the ICI generated by these adjacent subcarriers can be "self-cancelled" by each orther. This

scheme is also called polynomial cancellation (PCC). We will first analyze the ICI with single frequency as in [1],[2], and then show why the ICI self-cancellation works. The received signal on each subcarrier can be seen as a linear combination of signals received via different paths with different Doppler shifts. So that this scheme can also be used in the practical mobile environments that have significant Doppler spread.

The system architecture of the ICI self-cancellation scheme is shown in Figures 2.5-2.6. The only difference between the OFDM system with the ICI self-cancellation conventional scheme and the conventional OFDM system is the ICI self-canceling modulation/demodulation. We will show how this block works.
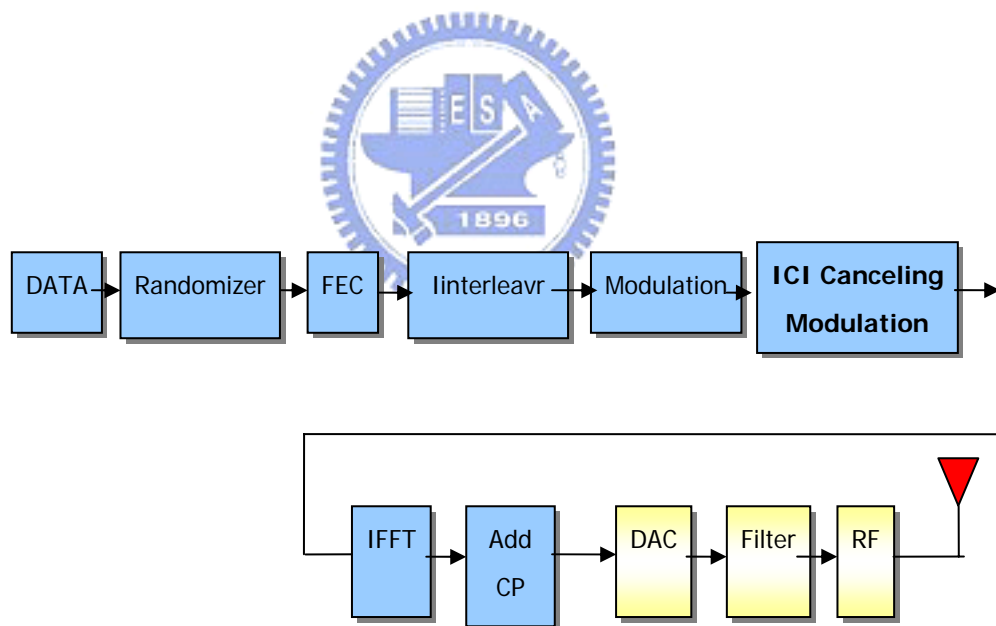
Figure2.5: Transmitter architecture of ICI self-cancellation scheme
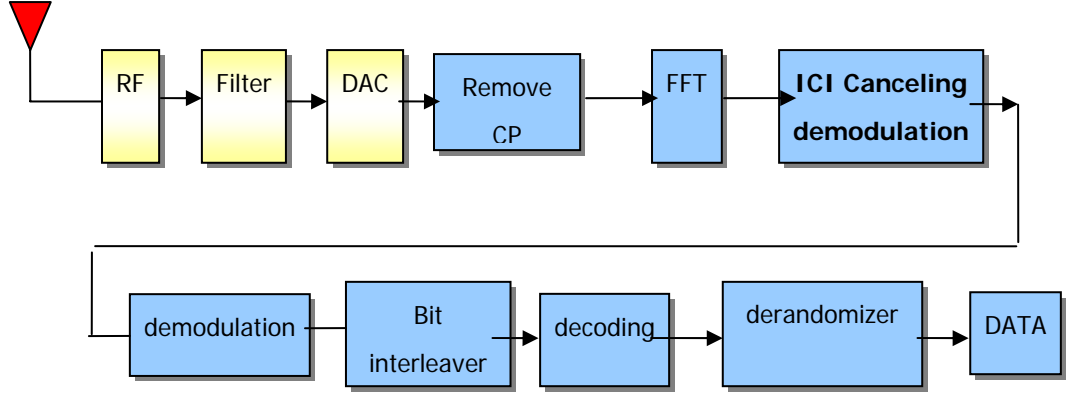
Figure2.6: Receiver architecture of ICI self-cancellation

Let the *n*-th OFDM transmission data be $x(n) = \frac{1}{N} e^{j2\pi f_c t} \sum_{m=0}^{N-1} s_m e^{j\frac{2\pi}{N}mn}$. In the receiver, we ignore the noise terms and assume that the signal is mixed with a local oscillator which has frequency mismatch Δf with the transmitter oscillator. Then the demodulated signal in the receiver before FFT can be written as $r(n) = \frac{1}{N} e^{j(2\pi\Delta ft+\theta)} \times \sum_{m=0}^{N-1} s_m e^{j\frac{2\pi}{N}mn}$, and assuming this signal is sampled at the optimum timing. After the sampling, the signal can be rewritten as

$$r(n) = \frac{1}{N} e^{j\theta} \times e^{j(2\pi n\Delta fT / N)} \times \sum_{m=0}^{N-1} s_k e^{j\frac{2\pi}{N}mn} \tag{2.22}$$

The sampled signal after DFT are given by

$$y(d) = \sum_{n=0}^{N-1} r_n e^{-j\frac{2\pi nd}{N}} \tag{2.23}$$

By Equations (2.22) and (2.23), we have the received signals after sampling and DFT

$$y(d) = \frac{1}{N} e^{j\theta} \times e^{j(2\pi n \Delta fT/N)} \sum_{n=0}^{N-1} \sum_{m=0}^{N-1} s_m e^{j\frac{2\pi}{N}mn} e^{j\frac{2\pi nd}{N}}$$

$$= \frac{1}{N} e^{j\theta} \times \sum_{n=0}^{N-1} \sum_{m=0}^{N-1} s_m e^{j\frac{2\pi n}{N}(m-d+\Delta fT)} \tag{2.24}$$

The analysis of ICI terms can be done by defining N complex weighting, $c_0 \cdots c_{N-1}$, which is the contribution of each input signal $s_0 \cdots s_{N-1}$.

$$y(d) = e^{j\theta} \sum_{m=0}^{N-1} c_{m-d} s_m \tag{2.25}$$

Compared Equations (2.24) with (2.25), we have the complex weighting written as

$$c_{m-d} = \frac{1}{N} e^{j\theta} \times \sum_{n=0}^{N-1} e^{j\frac{2\pi n}{N}(m-d+\Delta fT)}$$

$$= \frac{1}{N} \frac{\sin \pi (m-d+\Delta fT)}{\sin \pi (\frac{m-d+\Delta fT}{N})} e^{j\pi \frac{(N-1)(m-d++\Delta fT)}{N}} \tag{2.26}$$

By the aforementioned equation, we show the complex weighting value in Figure 2.7. The figure shows a smooth curve, this will be the key point why ICI self-cancellation works.

Zhao and Häggman have proposed a method to mitigate ICI called ICI self-cancellation scheme. This scheme maps the data tone onto adjacent subcarriers with different signs, such as $s_0 = -s_1, s_2 = -s_3, \ldots, s_{N-2} = -s_{N-1}$. The difference between the adjacent coefficients is small, and the adjacent subcarriers map to the same data with different signs. The ICI produced by adjacent subcarriers will be self-canceled by each other. The received signal after FFT can be written as

$$y(d) = \sum_{\substack{m=0 \\ m \in even}}^{N-2} s_m e^{j\theta} (c_{m-d} - c_{m+1-d})$$

$$y(d+1) = \sum_{\substack{m=0 \\ m \in even}}^{N-2} s_m e^{j\theta} (c_{m-k-1} - c_{m-d}) \tag{2.27}$$

In order to maximize the output SNR, the values $y(d)$, $y(d+1)$ should be subtracted in pairs as shown below

$$\breve{y}(d) = y(d) - y(d+1)$$

$$= \sum_{\substack{m=0 \\ m \in even}}^{N-2} s_m e^{j\theta} (c_{m-d} - c_{m+1-d})[2c_{m-d} - c_{m+1-d} - c_{m-k-1}] \tag{2.28}$$

where $\breve{y}(d)$ is the symbol that will be demodulated to obtain the information bits. By this way, the overall system SNR increases by a factor 2, due to the coherent addition.
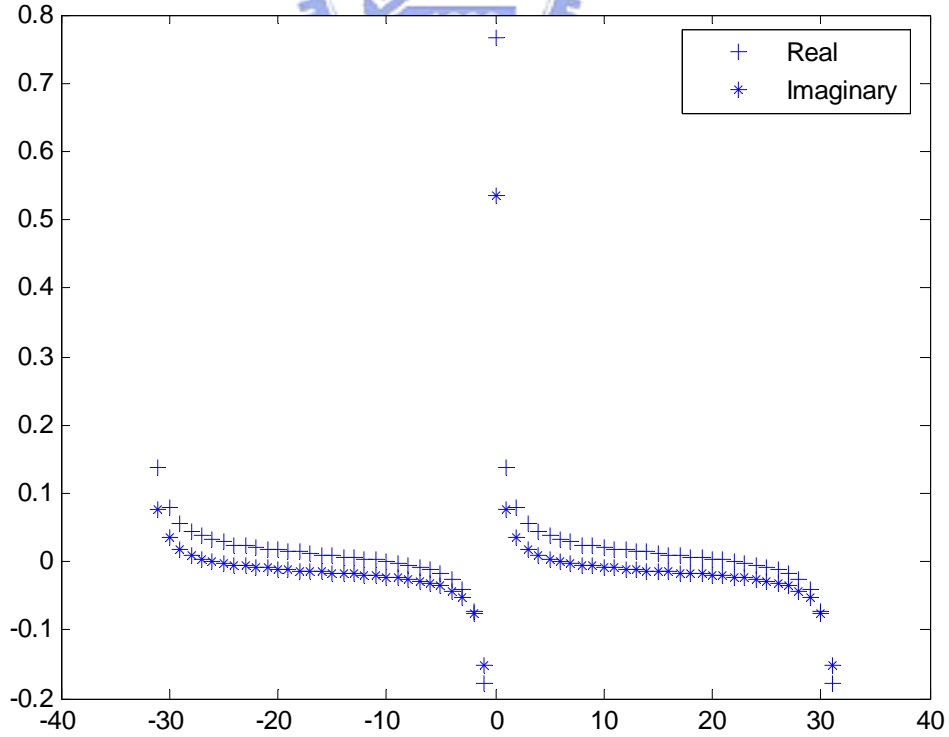
Figure2.7: ICI cofficients of different subcarriers

A disadvantage of this system is that its bandwidth efficiency is only half of the conventional OFDM system. There are some new researches to improve the bandwidth efficiency, such as in [13]. We only show that ICI self-cancellation scheme can self cancel the ICI produced by a frequency error due to mismatch between the transmitter and receiver oscillators in the above description. In real mobile environments, the received signal on each subcarrier can be seen as a linear combination of signals received via different paths with different Doppler shifts. So this scheme can also be used in the practical mobile environments that have significant Doppler spread.

2.3.2 Frequency Domain Equalizer Scheme

Frequency domain equalizer is a method which is used frequently in compensating the ICI of OFDM systems in mobile environments. The transmitter architecture is the same as conventional OFDM system. Besides, a frequency domain equalizer after FFT is added as shown in Figure 2.8. The signals of OFDM systems in the receiver before FFT are usually called the "Time Domain Signals", and those after FFT are called the "Frequency Domain Signal". By this definition, the frequency domain equalizer equalizes the received signal after FFT. There are many equalizers technique can be used here with different performance and complexity, such as block minimum mean square equalizer (MMSE) or block Zero-forcing (ZF), FIR equalizer, etc. The block of MMSE and ZF equalizer is shown below.

$$W_{MMSE} = (H^H H + \frac{\sigma_\eta^2}{\sigma_s^2} I_N)^{-1} H^H \tag{2.29}$$

$$W_{ZF} = (H^H H)^{-1} H^H \tag{2.30}$$

where W is the equalizer weighting, H is the channel matrix in time domain, σ_η^2 is the noise power, and σ_s^2 is the signal power. Some low-complexity equalizers have already been proposed, as in [3], [4], [5], [6], [7]. This paper also proposed a low-complexity technique based on the block MMSE equalizer and will be shown in Chapter 4.
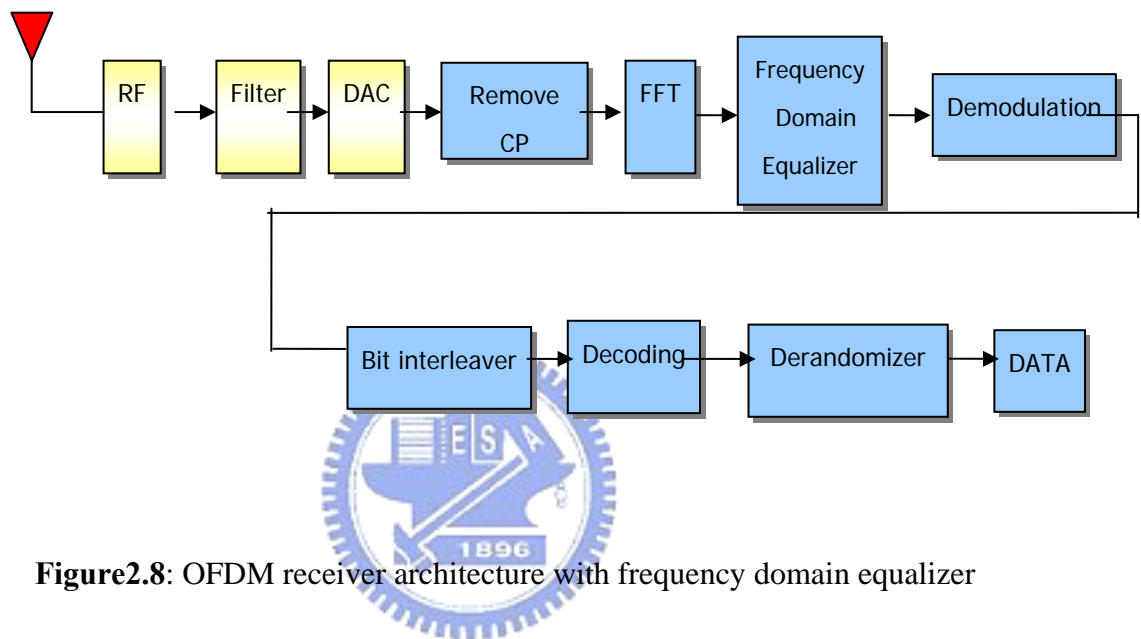
Figure2.8: OFDM receiver architecture with frequency domain equalizer

2.4 Summary

In this chapter, we first introduce the traditional OFDM system, and show the challenges to the OFDM system over time-varying channels. In particular, the ICI is the major subject of interest. We also introduce some existing techniques for solving this problem, such as the ICI self-cancellation schemes and the frequency domain equalizer schemes. Finally, modified OFDM systems for time-varying channel are presented.

Chapter 3

Introduction to Conjugate Gradient (CG) Algorithm

We will first show the basic concept of projection and then introduce the Krylov subspace and some krylov subspace methods that are the predecessor of conjugate gradient methods. The evolution from basic Krylov method to conjugate gradient method is shown in Section 3.4. The Krylov subspace method is currently to be the most important iterative technique for solving large linear systems, and the CG algorithm is a mature algorithm in this topic.

3.1 Projection Methods

We will first show the general projection theory [9], [10] and then show the projection can minimize error between the real solution and the approximate solution obtained by the projection methods.

3.1.1 General Projection

Most of the existing practical iterative techniques for solving linear systems utilize a projection method. A projection method can be seen as a scheme of extracting an approximate solution of a linear system from a subspace. We call this subspace the search subspace or the candidate approximants denote by K. Assume that it has the dimension n. In general, there should have n constraints be imposed to be exacting the approximate solution. A typical way of these constraints is l independent conditions. We define a subspace L, which is called the subspace of constraints or left subspace. There are two kinds of projection methods, orthogonal and oblique. An orthogonal projection means that the subspace L is the same as K. The oblique projection means that the subspace L is different from K, and they can have some relationships or be totally uncorrelated.

We show the mathematically approach of projection the technique. A projection technique onto the subspace can obtain approximated solution $\hat{x}$ by

$$\text{Search } \hat{x} \in K \quad \text{and} \quad b - A\hat{x} \perp L \tag{3.1}$$

or with initial guess x_0

$$\text{Search } \hat{x} \in x_0 + K \quad \text{and} \quad b - A\hat{x} \perp L \tag{3.2}$$

Defining the initial residual vector r_0 as $r_0 = b - Ax_0$, then Equation (4.2) can be written as

$$\hat{x} = x_0 + \sigma, \sigma \in K$$

$$(r_0 - A\sigma, q) = 0, \ \forall \ q \in L \tag{3.3}$$

Let $P = [p_1, \ldots p_n]$ be a basis of K, and $Q = [q_1, \ldots q_n]$ be a basis of L. Then the approximate solution in Equation (4.3) can be written as

$$\hat{x} = x_0 + Py \tag{3.4}$$

By $b - Ax = b - Ax_0 - AVy$ and $Q^T(b - Ax) = 0$, we have

$$y = (Q^T AP)^{-1} Q^T r_0 \tag{3.5}$$

By Equations (4.4) and (4.5), we have the projection method based on Equation (4.2) in the matrix form, which is

$$\hat{x} = x_0 + P(Q^T AP)^{-1} Q^T r_0 \tag{3.6}$$

3.1.2 Property of the Projection Method

We will show that orthogonal projection solution can minimize the error between the desired solution and the approximate solution as in [9]. Let P is the orthogonal projector onto a subspace K, x is the desired vector, and y is the arbitrary vector in subspace K. Because of the orthogonality between x and Px, we have

$$\|x - y\|_2^2 = \|x - Px + Px - y\|_2^2 = \|x - Px\|_2^2 + \|Px - y\|_2^2, \ y \in K \tag{3.7}$$

Therefore, $\forall y \in K, \|x - y\|_2 \geq \|x - Px\|_2$, we know that the orthogonal projection can minimize 2-norm error between x and y. Let y' is the orthogonal projection from x onto subspace K, and then we have

$$\begin{aligned} y' &\in K \\ x - y' &\perp K \end{aligned} \tag{3.8}$$

If A is a symmetric and positive definite matrix, we can derive the similar result that orthogonal projection can minimize A-norm error between x and y. By Equation (4.6), we have

$$(A(x - y'), q) = 0, \ \forall \ q \in K \tag{3.9}$$

25

By $Ax = b$, Equation (4.7) can be rewritten as

$$(b - Ay', q) = 0 , \ \forall \ q \in K \tag{3.10}$$

This is called the Galerkin condition which defines an orthogonal projection [9].

Let A is an arbitrary matrix, and $L = AK$. The oblique projection onto K and orthogonal to L will minimize the 2-norm of the residual vector $r = b - A\hat{x}$. The derivation is similar as the orthogonal projection. Then we have

$$(b - Ay', v) = 0 , \ \forall \ v \in AK \tag{3.11}$$

This is called the Petrov-Galerkin condition which defines an oblique projection [9].

3.2. Overview of Krylov Subspace

The Krylov subspace is a subspace of the form [8],[9],[10]

$$K^m(A, r_0) = \mathrm{span}\{r_0, Ar_0, A^2 r_0 \dots, A^{m\text{-}1} r_0\} \tag{3.12}$$

By this definition, we know that K^m is the subspace of all vectors in $\mathbb{R}^n$ that can be written as $x = polynomial(A) * r_0$ and the degree of polynomial do not exceed r_0 .

We will show the iterative methods are located in the Krylov subspace. Solving $Ax = b$, we may solve the simplified system $Tx_0 = b$ first. Then x_0 is an approximate solution for x . We may correct the approximation x_0 with δ , so δ should satisfy

$$A(x_0 + \delta) = b \tag{3.13}$$

This can be seen as a new linear system

$$A\delta = b - Ax_0 \tag{3.14}$$

We may solve Equation (3.13) by a simplified approximate system

$$T\delta = b - Ax_0 \tag{3.15}$$

Then the new approximate solution will be $x_1 = x_0 + z_0$. We may again correct the approximate solution with the same process respect to x_1. Therefore, we have

$$
\begin{aligned}
x_{i+1} &= x_i + \delta \\
&= x_i + T^{-1}(b - Ax_i)
\end{aligned}
\tag{3.16}
$$

By setting $T = I$, the Equation (3.13) can be written as

$$x_{i+1} = x_i + (b - Ax_i) = b + (I - A)x_i = x_i + r_i \tag{3.17}$$

Multiplying Equation (3.16) by $-A$ and adding b, we have

$$b - Ax_{i+1} = b - Ax_i - Ar_i \tag{3.18}$$

that is the same as

$$r_{i+1} = (I - A)r_i = (I - A)^{i+1}r_0 = p_{i+1}(A)r_0 \tag{3.19}$$

By $\|r_{i+1}\| \le \|I - A\|\|r_i\|$, this result shows that we have guaranteed the convergence for any initial r_0 if $\|I - A\| \le 1$ Assuming that A has n eigenvectors a_i with corresponding eigenvectors λ_j, we write the initial residual r_0 as

$$r_0 = \sum_{i=1}^{n} \xi_i a_i \tag{3.20}$$

By Equation (3.16), we have

$$r_i = p_i(A)r_0 = \sum_{i=1}^{n} \xi_i p_i(\lambda_i)a_i \tag{3.21}$$

Equation (3.18) shows that the residual of the system depends on how well the polynomial p_i damps the initial error.

By Equation (3.14), the *i*-th approximate solution x_i can be expressed as

$$x_i = x_0 + r_0 + r_1 + \ldots + r_{i-1}$$

$$= x_0 + \sum_{k=0}^{i-1} (I - A)^k r_0$$

$$\in span\{x_0, r_0, A r_0 \ldots A^{i-1} r_0\} \equiv K^i(A, r_0) \tag{3.22}$$

The aforementioned discussion shows that iterative methods are located in the Krylov subspace. By different definitions of K and L (see Section 3.1), different projection methods can be obtained, such as orthogonal or oblique projection, and different kinds of iterative techniques have been derived. They have different convergence rates. One should choose the best iterative method on a case by case basis. Usually, the characteristic of A plays an important role in choosing the appropriate iterative method. Choosing an appropriate method can have significant improvement on the convergence rate and the complexity.
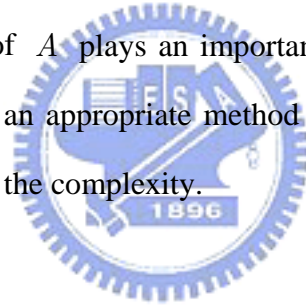
3.3 Krylov Subspace Methods

There are many kinds of Krylov subspace methods, and we focus on the predecessor of CG methods, and the CG method. We will show the evolution from the basic projection, the Arnoldi's method, and then derive other simplified methods: the symmetric Lanczos algorithm and the CG algorithm.

3.3.1 Arnoldi's Algorithm

Arnoldi's algorithm is a basic orthogonal projection method. This scheme was first introduced in 1951 by Arnoldi. This is a method that builds an orthogonal basis of

the Krylov subspace and finds an approximate solution on the Krylov subspace by orthogonal projection. The basic Arnoldi's algorithm can be found in [9]

Algorithm 3.1 Arnoldi's Algorithm

Choose a vector p_1, $\|p_1\| = 1$

for $j = 1 \sim m$

for $i = 1 \sim j$

$h_{ij} = (Ap_j, p_i)$, $b_j = Ap_j - \sum_{i=1}^{j} h_{ij} p_i$

$h_{j+1,j} = \|w_j\|^2$

If $h_{j+1,j} = 0$, Stop   Else $p_{j+1} = w_j / h_{j+1,j}$

The above process builds an orthogonal basis by a Gram-Schmidt process. The above algorithm can be rewritten in the matrix form as

$$Ap_j = \sum_{i=1}^{j} h_{ij} p_i + b_j = \sum_{i=1}^{j} h_{ij} p_i + h_{j+1,j} p_{j+1} = \sum_{i=1}^{j+1} h_{ij} p_i \tag{3.23}$$

Assuming P_m is the $n \times m$ matrix containing the m vectors that forms an orthogonal basis of the Krylov subspace. We can rewrite Equation (3.22) in the matrix form as

$$AP_m = P_{m+1} \dot{H}_m \tag{3.24}$$

$$P_m^T AP_m = H_m \tag{3.25}$$

where $\dot{H}_m$ has the form

$$
\dot{H}_m = \begin{bmatrix} h_{11} & h_{12} & h_{13} & \cdots & h_{1m} \\ h_{21} & h_{22} & h_{23} & \cdots & h_{2m} \\ 0 & h_{32} & h_{33} & \cdots & \vdots \\ \vdots & 0 & h_{43} & \ddots & \vdots \\ \vdots & \vdots & 0 & \ddots & h_{mm} \\ 0 & 0 & \vdots & 0 & h_{m+1,m} \end{bmatrix}_{(m+1) \times m}
\tag{3.26}
$$

H_m is a Hessenberg matrix obtained by deleting the last row in $\dot{H}_m$.

The above process produces an orthogonal basis of the Krylov subspace. By Equations (3.4) and (3.5), orthogonal projection means that the subspace L is the same as K. We have

$$
x_m = x_0 + Py
\tag{3.27}
$$

$$
y = (P^T A P)^{-1} P^T r_0 = H_m^{-1}(\|r_0\|_2 e_1)
\tag{3.28}
$$

Combining Equations (3.26) and (3.27), we have the equation for orthogonal projection onto Krylov subspace as

$$
x_m = x_0 + P_m H_m^{-1}(\|r_0\|_2 e_1)
\tag{3.29}
$$

3.3.2 Krylov Subspace Methods Based on Arnoldi's Algorithm

A method is called the **full orthogonalization method** (FOM) that searches the orthogonal basis of the Krylov subspace by Arnoldi's theorem and finds the approximate solution by Equation (3.28). There are some modified methods that have lower complexity than the FOM method. **Restarted FOM** is to restart the Arnoldi's algorithm periodically. **Incomplete orthognoalization process** (IOM) is to truncate

the bases generated by the original Arnoldi's algorithm. We find the new basis only orthogonal to several bases that have already been found.

Algorithm 3.2 IOM Algorithm
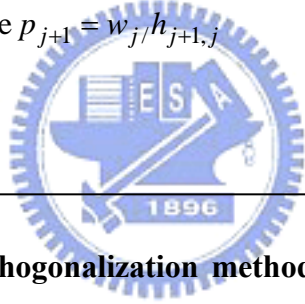
Choose a vector p_1, $\|p_1\| = 1$

for $j = 1 \sim m$

for $i = 1 \sim \max(1, j\text{-}t+1)$

$$h_{ij} = (Ap_j, p_i), b_j = Ap_j - \sum_{i=1}^{j} h_{ij} p_i$$

$$h_{j+1,j} = \left\| w_j \right\|^2$$

If $h_{j+1,j} = 0$, Stop   Else $p_{j+1} = w_j / h_{j+1,j}$

$$\hat{x} = x_0 + P_m H_m^{-1} (\|r_0\|_2 e_1)$$

Direct incomplete orthogonalization method (DIOM) derived from IOM is a progressive method in solving the approximate solution. Based on the above algorithm, the Hessenberg matrix H_m in Equation (3.24) will be a band matrix with upper bandwidth equal to $t-1$ and lower bandwidth equal to 1, which can be shown as follows

$$H_m = \begin{bmatrix} h_{11} & \ldots & h_{1t} & 0 & \ldots & & 0 \\ h_{21} & h_{22} & \ldots & h_{2t} & 0 & & \vdots \\ 0 & h_{32} & h_{33} & \ldots & \ddots & & 0 \\ \vdots & 0 & h_{43} & \ldots & & \ddots & h_{(m-t+1),m} \\ \vdots & \vdots & 0 & \ddots & \ddots & & \vdots \\ 0 & 0 & \vdots & 0 & h_{m,(m-1)} & & h_{mm} \end{bmatrix}_{m \times m} \tag{3.30}$$

Take the LU factorization of this matrix. Because H_m is a Hessenberg band matrix with bandwidth equal to $t+1$, its LU factorization will have the form that the lower triangle matrix is a unit band lower triangle matrix, and the upper triangle matrix has upper bandwidth equal to $t-1$. These two matrices are shown below.

$$L_m = \begin{bmatrix} 1 & 0 & \cdots & & \cdots & 0 \\ l_{21} & 1 & 0 & & \cdots & 0 \\ \vdots & l_{22} & \ddots & & 0 & \vdots \\ \vdots & 0 & \ddots & & \ddots & 0 \\ 0 & \vdots & 0 & & l_{m,m-1} & 1 \end{bmatrix}_{m \times m}$$

$$U_m = \begin{bmatrix} u_{11} & \cdots & u_{1k} & 0 & \cdots & & 0 \\ 0 & u_{22} & \cdots & h_{2t} & 0 & & \vdots \\ \vdots & 0 & u_{33} & \cdots & & \ddots & 0 \\ \vdots & \vdots & 0 & \cdots & & \ddots & u_{(m-t+1),m} \\ \vdots & \vdots & \vdots & & \ddots & & \vdots \\ 0 & 0 & 0 & 0 & 0 & & u_{mm} \end{bmatrix}_{m \times m} \tag{3.31}$$

Then Equation (3.28) can be written as

$$x_m = x_0 + P_m H_m^{-1}(\|r_0\|_2 e_1) = x_0 + P_m U_m^{-1} L_m^{-1}(\|r_0\|_2 e_1) \tag{3.32}$$

We define $G_m = P_m U_m^{-1}$, $c_m = L_m^{-1}(\|r_0\|_2 e_1)$, then Equation (3.31) can be rewritten as

$$x_m = x_0 + G_m c_m \tag{3.33}$$

By the definition of G_m and $G_m U_m = P_m$, let $g_1 \sim g_m$ be the columns of G_m and we have

$$\sum_{k=m-t+1}^{t-1} u_{km} g_k + u_{mm} g_m = p_m \tag{3.34}$$

The above equation can be rewritten as

$$g_m = \frac{1}{u_{mm}} \left(p_m - \sum_{k=m-t+1}^{t-1} u_{km} g_k \right) \tag{3.35}$$

By the definition of c_m, we have

$$c_m = \begin{bmatrix} c_{m-1} \\ -\eta_m \end{bmatrix}$$ (3.36)

where $\eta_m = l_{m,m-1}\eta_{m-1}$

By Equation (3.32), we have the iterative equation as

$$\begin{aligned}
x_m &= x_0 + G_m c_m \\
&= x_0 + G_{m-1}c_{m-1} + \eta_m g_m \\
&= x_{m-1} + \eta_m g_m
\end{aligned}$$ (3.37)

In FOM and IOM algorithm, we require an orthogonal basis to solve the approximate solution. By Equation (3.36), we have a progressive method to solve x_m, which can solve the projection problem iteratively. Finally we have the DIOM algorithm which is mathematically identical to the IOM algorithm, but a progressive version.

Algorithm 3.3 DIOM Algorithm

Choose a vector p_1

for $j = 1 \sim m$

   for $i = 1 \sim \max(1, j\text{-}t+1)$

   $h_{ij} = (Ap_j, p_i), b_j = Ap_j - \sum_{i=1}^{j} h_{ij}p_i$

   $h_{j+1,j} = \|w_j\|^2$, If $h_{j+1,j} = 0$, Stop   Else $p_{j+1} = w_j/h_{j+1,j}$

   $g_m = \dfrac{1}{u_{mm}}(p_m - \sum_{k=m-t+1}^{t-1} u_{km}g_k)$

   $\eta_0 = \|p_1\|, \quad \eta_m = l_{m,m-1}\eta_{m-1} \quad x_m = x_{m-1} + \eta_m g_m$

3.3.3 Symmetric Lanczos Algorithm

The symmetric Lanczos algorithm is a simplified Arnoldi's method in which the matrix is symmetric. When solving $Ax = b$ in the assumption that A is symmetric matrix, the Hessenberg matrix H_m in Equation (3.24) is also a symmetric matrix, hence it is a tridiagonal matrix. We can reduce the computational complexity by this characteristic. A three-term recurrence equation can be found based on the Arnoldi's algorithm.

The Hessenberg matrix H_m in Equation (3.24) should have the structure as follows

$$H_m = \begin{bmatrix} a_1 & b_2 & & \\ b_2 & a_2 & & \\ & & \ddots & b_m \\ & & b_m & a_m \end{bmatrix}_{m \times m} \tag{3.38}$$

Then the Arnoldi's theorem can be simplified to the Lanczos Algorithm as in [8]

Algorithm 3.4 Lanczos method

Choose a vector p_1, $\|p_1\| = 1$

for j=1~m

$t_j = Ap_j - b_j p_{j-1}$, $a_j = (Ap_j, p_i)$

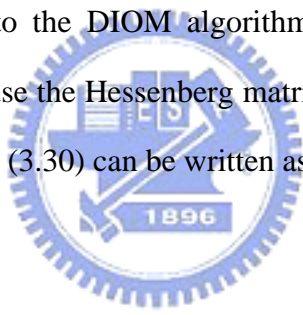$t_j = t_j - a_j p_j$, $b_{j+1} = \|w_j\|^2$

If $b_{j+1} = 0$, Stop else $p_{j+1} = w_j / b_{j+1}$

Then we can find the orthogonal basis of the Krylov subspace by Lanczos's theorem, and find the approximate solution by Equation (3.28), if A is symmetric. This process will require fewer computations than the Arnoldi's method.

3.3.4 Conjugate Gradient Method

Like the FOM algorithm in the assumption that A is symmetric, we can build an orthogonal basis based on the Lanczos algorithm. Then we can use Equation (3.28) to find orthogonal projection onto the Krylov subspace which is the desired approximate solution.

An algorithm similar to the DIOM algorithm can be derived. It is called the D-Lanczos algorithm. Because the Hessenberg matrix H_m is a tridiagonal matrix, the LU factorization in Equation (3.30) can be written as

$$L_m = \begin{bmatrix} 1 & 0 & \cdots & 0 \\ r_1 & 1 & \ddots & \vdots \\ 0 & \ddots & \ddots & 0 \\ \vdots & 0 & r_m & 1 \end{bmatrix}_{m \times m}$$

$$U_m = \begin{bmatrix} h_1 & o_1 & 0 & \cdots \\ 0 & h_2 & \ddots & 0 \\ \vdots & 0 & \ddots & o_n \\ 0 & \vdots & 0 & h_m \end{bmatrix}_{m \times m} \tag{3.39}$$

By Equation (3.38), Equation (3.32) can be simplified to

$$h_m g_m + o_m g_{m-1} = p_m \tag{3.40}$$

Equation (3.39) can be rewritten as

$$g_m = \frac{1}{h_{mm}}(p_m - o_m g_m) \tag{3.41}$$

Then we have the D-Lanczos algorithm by replacing the equation of computing g_m in DIOM algorithm (algorithm 3.3) with Equation (3.40). Because the approximate solution is iteratively found by

$$x_m = x_{m-1} + \alpha_m g_m \tag{3.42}$$

where g_m is called the searching direction vector. The CG method can be derived from the D-Lanczos algorithm by two properties. The first is that the residual vectors are orthogonal to each other and the second is that the search direction vectors g_m are A-conjugate that is $(Ag_i, g_j) = 0, \ \forall i \neq j$.

The residual vector can be written as

$$\begin{aligned} r_m &= Ax_m - b = A(x_{m-1} + \eta_{m-1}g_{m-1}) - b \\ &= r_{m-1} - \eta_{m-1}Ag_{m-1} \end{aligned} \tag{3.43}$$

And the search direction vector p_m can be found by

$$g_m = r_m + \xi_{m-1}g_{m-1} \tag{3.44}$$

The coefficients ξ_{m-1} and η_m can be found by the aforementioned two properties. Finally, we have the CG algorithm, which is one of the best known iterative techniques in solving the symmetric positive definite (S.P.D) system.

Algorithm 3.5 Conjugate gradient method

$r_0 = b - Ax_0, \; g_0 = r_0$

for j=0~convergence

$\alpha_j = (r_j, r_j)/(Ag_j, g_j) = r_j^T r_j \big/ g_j^T Ag_j,$

$x_{j+1} = x_j + \alpha_j g_j \; \; r_{j+1} = r_j - \alpha_j Ag_j$

$\beta_j = (r_{j+1}, r_{j+1})/(r_j, r_j) = r_{j+1}^T r_{j+1} \big/ r_j^T r_j \; \; g_{j+1} = r_{j+1} + \beta_j g_j$

3.5 Summary

In this chapter, we first introduce the concept of projection and derive the CG algorithm from basic projection theory. CG algorithm is one of the best known iterative techniques for solving a symmetric positive definite (S.P.D) system. We will use the PCG algorithm for solving the matrix inverse problem in the MMSE equalizer in the next chapter.
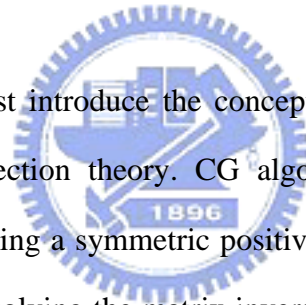
Chapter 4

Proposed Low-Complexity Frequency Domain Equalizer

The frequency domain equalizer schemes are introduced briefly in Chapter 2. In this chapter, the band channel approximation based on the previous analysis is shown in the first place. By this approximation, some techniques have been proposed to reduce the complexity of different equalizers as introduced in Section 4.2. In addition, an MMSE equalizer based on the CG method with optimal preconditioning is proposed. And then we compare the complexity of this scheme with some other methods. Finally, performance simulations are shown in Section 4.5

4.1 Band Channel Approximation

The magnitude of the frequency domain channel matrix is shown in Figure 4.1. The channel model is the Jakes model and the normalized Doppler spread equals 0.1. It is shown that the most significant coefficients are those on the central band and the edges of the matrix, which is similar to the analysis of the channel in Chapter 2. In order to reduce the computation complexity, the smaller coefficients are ignored and only the significant coefficients are dealt with. Although there are some losses in the

BER performance, the computation complexity of mobile OFDM systems can be reduced greatly.

The frequency domain channel can be approximated as in Figure 4.2, [5], [6]. We can only take account of the coefficients in the shaded region and ignore other coefficients. Then a frequency domain channel matrix with bandwidth Q as shown in Figure 4.2 is processed. A time-domain technique discussed in [6] can enhance this approximation.
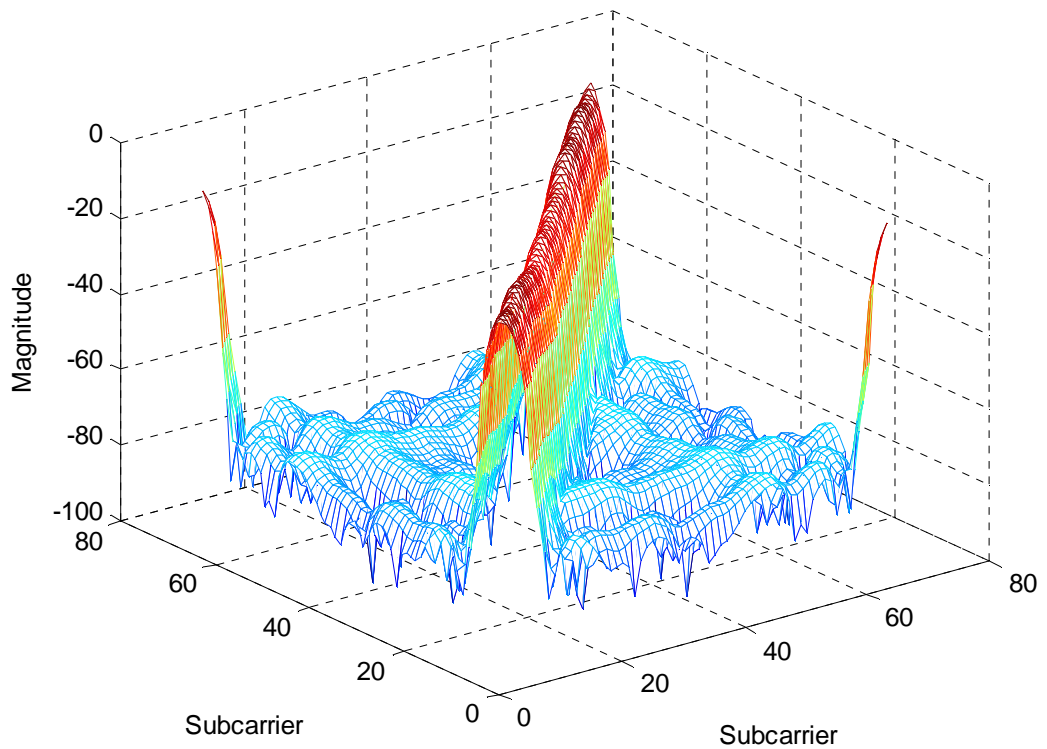

Figure 4.1: Amplitude of frequency domain channel matrix in Jakes model
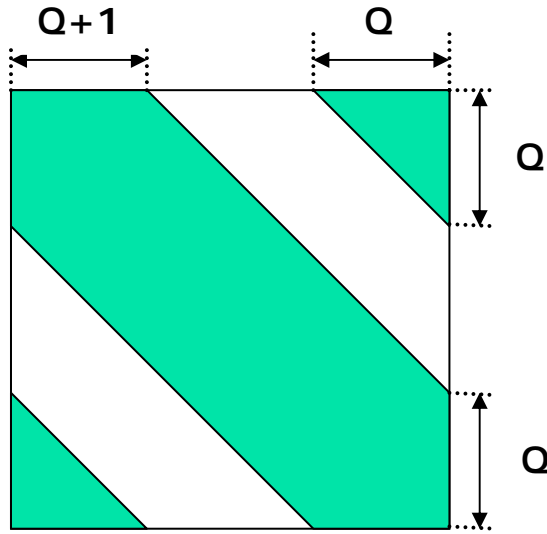
Figure 4.2: Structure of approximate frequency domain channel

4.2 Existing Low-Complexity Frequency Domain Equalizers

Two important low-complexity frequency domain equalizers will be introduced, which are proposed in [4], [6]. The main ideas behind them are also the band channel approximation. We adopt the mobile OFDM signal model introduced in Chapter 2, Equation (2.17), and ignore the superscript (i) giving

$$
\begin{aligned}
\mathbf{y} &= \mathbf{Fr} = \mathbf{FHx} + \mathbf{F\eta} \\
&= \mathbf{FHF}^H \mathbf{s} + \mathbf{F\eta} = \mathbf{As} + \mathbf{z}
\end{aligned}
\tag{4.1}
$$

A linear minimum mean square equalizer (LMMSE) can be used to equalize the received signal. The weight computations are based on

$$
\mathbf{W}_{mmse} = \arg\ \min_{\mathbf{W}}\ \mathrm{E}\{\left\| \mathbf{W}^H \mathbf{y} - \mathbf{s} \right\|^2 \}
\tag{4.2}
$$

It can be easily derived that the optimum weights in the above equation are

$$\mathbf{W}_{mmse} = (\mathbf{A}\mathbf{A}^H + \frac{1}{\mathbf{SNR}}\mathbf{R}_{zz})^{-1}\mathbf{A} \tag{4.3}$$

where $\mathbf{A} = \mathbf{FHF}^H$ is the equivalent channel in the frequency domain as shown in Equation (4.1), and $\mathbf{R}_{zz}$ is the autocorrelation matrix of the noise. The equalized signal can be written as $\mathbf{d} = \mathbf{W}_{mmse}^H \mathbf{y}$, and then the receiver make decision based on this equalized signal. In Equation (4.3), an $N \times N$ matrix inversion is required. It requires $O(N^3)$ computations which is too expensive to be realized for a large N. One should apply a low complexity algorithm to solve this problem.

By the idea that the ICI only comes from the neighborhood subcarriers, Xiaodong Cai and Georgios B. Giannakis proposed a low-complexity LMMSE equalizer in [4], Assuming that $\mathbf{s}_i$ is the desired signal to be solved, it can only take the $2Q+1$ rows of the $\mathbf{A}$ matrix for computing the LMMSE weight vector. It means we are only concerned with the ICI coming from the $2Q$ neighborhood subcarriers, and ignore the ICI produced by the subcarriers out of the $2Q$ neighborhood, as shown in Figure 4.3. Because the significant parts of the ICI come from the neighborhood subcarriers, this assumption is meaningful.

The $2Q+1$ rows of $\mathbf{A}$ matrix for calculating the LMMSE weight vector for $\mathbf{s}_i$ is $\mathbf{A}_i = \mathbf{A}((i-Q+1+j),:), j=1,\ldots 2Q+1$, let $\mathbf{y}_i = \mathbf{y}(i-Q+1+j), j=1,\ldots 2Q+1$, $\mathbf{z}_i = \mathbf{z}(i-Q+1+j), j=1,\ldots 2Q+1$, Equation (4.1) can be rewritten as

$$\mathbf{y}_i = \mathbf{A}_i\mathbf{s}_i + \mathbf{z}_i \tag{4.4}$$

Therefore the equation for computing the LMMSE weights from Equations (4.3) and (4.4) can be written as

$$\mathbf{w}_{mmse,i} = (\mathbf{A}_i\mathbf{A}_i^H + \frac{1}{\mathbf{SNR}}\mathbf{R}_{zi})^{-1}\mathbf{A}_i \tag{4.5}$$

where

$$\mathbf{A}_i = \begin{bmatrix} A(i-Q,1) & \cdots & A(i-Q,i) & \cdots & A(i-Q,N) \\ \vdots & \ddots & \vdots & \ddots & \vdots \\ A(i+Q,1) & \cdots & A(i+Q,i) & \cdots & A(i+Q,N) \end{bmatrix}_{(2Q+1)\times(N)} \qquad (4.6)$$

is a part of the original channel matrix, $\mathbf{R}_{zi}$ is a part of the autocorrelation function. This technique can be seen as partitioning a large system into several small systems, which can be easily solved. Note that the last $2Q$ rows of the matrix $\left(\mathbf{A}_i\mathbf{A}_i^H + \frac{1}{SNR}\mathbf{R}_{zi}\right)$ in Equation (4.5) is the same as first $2Q$ rows of the matrix $\left(\mathbf{A}_{i+1}\mathbf{A}_{i+1}^H + \frac{1}{SNR}\mathbf{R}_{z(i+1)}\right)$. The inverse can be calculated recursively as in [4]. Because the step of computing $\mathbf{A}_i\mathbf{A}_i^H$ requires at least $O(N^2)$ computations, this algorithm also requires $O(N^2)$ computations to solve the LMMSE problem.
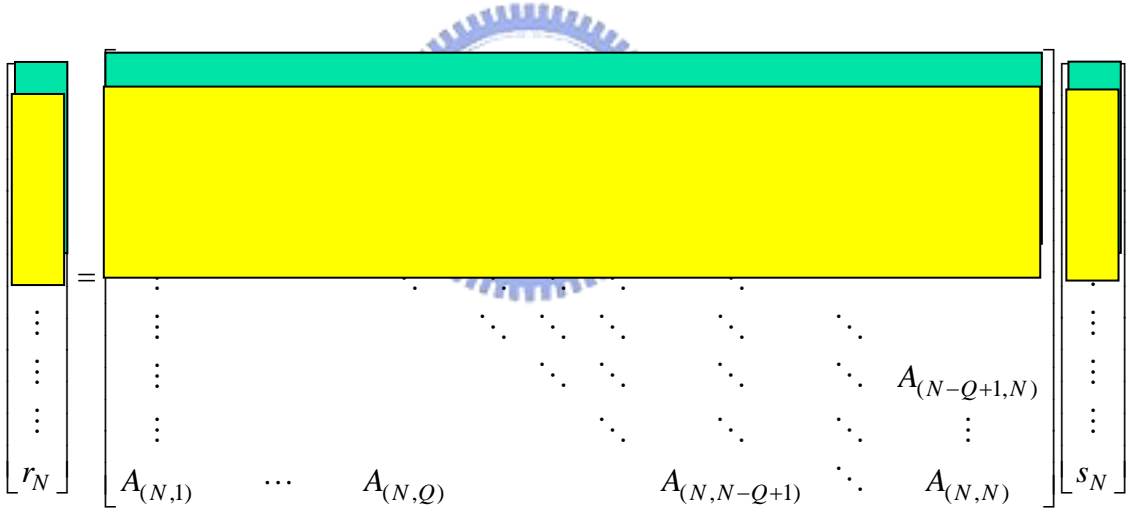

Figure 4.3: MMSE equalizer (proposed by Xiaodong Cai and Georgios B. Giannakis)

Another similar approach is proposed by Philip Schniter in [6]. We call this scheme the Partial MMSE equalizer for simplicity. This method applies the band channel approximation as described in Section 4.1. Assume that we want to retrieve the signal $\mathbf{s}_i$. We define

$$\mathbf{A}'_i = \begin{bmatrix} A(i-Q,i-2Q) & \cdots & A(i-Q,i) & 0 & & \cdots \\ 0 & \ddots & \vdots & \ddots & \\ \vdots & & A(i+Q,i) & \cdots & A(i+Q,i+2Q) \end{bmatrix}_{(2Q+1)\times(4Q+1)} \tag{4.7}$$

Then the size of the matrix to deal with can be reduced to $(2Q+1)\times(4Q+1)$ rather $(2Q+1)\times(N)$ in the first method. The system can be rewritten as in Equation (4.4) with $\mathbf{A}_i$ replaced by $\mathbf{A}'_i$ in Equation (4.6), and the LMMSE equalizer can also be applied. The computation of LMMSE weights is similar to Equation (4.5) as follows

$$\mathbf{w}'_{mmse,i} = (\mathbf{A}'_i \mathbf{A}'^H_i + \frac{1}{\mathbf{SNR}} \mathbf{R}_{zi})^{-1} \mathbf{A}'_i \tag{4.8}$$

Because it only requires $O(N)$ computations to compute $\mathbf{A}'_i \mathbf{A}'^H_i$, this algorithm requires $O(N)$ computations to solve the LMMSE problem.
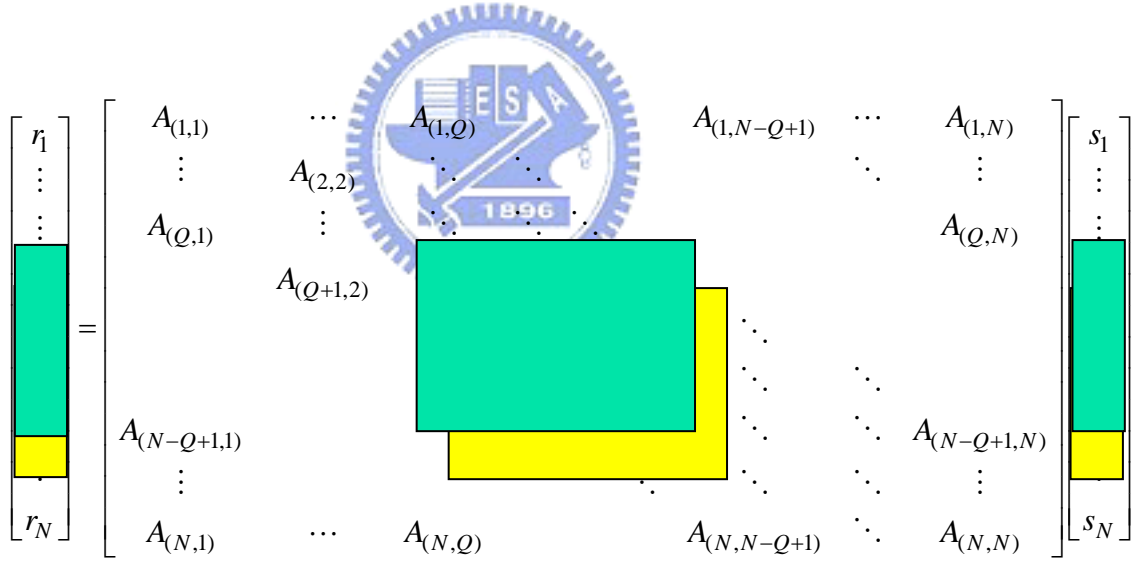

Figure 4.4: Partial MMSE eqaulizer (proposed by Philip Schniter)

4.3 Proposed Preconditioned Conjugate Gradient (PCG) MMSE Equalizer

In this section, a low-complexity LMMSE equalizer by using preconditioned conjugate gradient algorithm for solving the matrix inversion problem is proposed. It will be shown that the complexity of this method is $O(N)$ and have similar performance but further computations than Partial MMSE equalizer.

4.3.1 Preconditioned Conjugate Gradient (PCG) Algorithm

One of the serious defects of iterative methods is the lack of robustness. CG works regularly if the system is well conditioned. Because CG is a project technique to the Krylov subspace K^m which is the subspace of $\mathbb{R}^n$, it will converge in at most n iteration. The convergence rate of CG is related to the condition number κ which is defined as follows

$$\kappa = \frac{\lambda_{\max}}{\lambda_{\min}} \tag{4.9}$$

where $\lambda_{\max}$ and $\lambda_{\min}$ are the maximum and minimum eigenvalue of the A matrix. If the condition number is large, the CG algorithm will converge slowly. This characteristic limits the application of CG algorithm. However, if some statistical characteristic of A is known, it can be utilized to achieve faster convergence rate and then the system will be more robust. This is the idea of preconditioning which is a technique to better the condition number of the system.

Assuming M is the precondition matrix. Then the basic precondition method is to solve the system $M^{-1}Ax = M^{-1}b$ instead of $Ax = b$. Therefore, the system

convergence rate depends on the condition number of the preconditioned system $M^{-1}A$. If M is chosen appropriately, the condition number of $M^{-1}A$ can be smaller than the original matrix A. For this reason, solving the system $M^{-1}Ax = M^{-1}b$ will converge quickly.

There are some criteria for choosing the precondition matrix M, which is introduced in [8], [9], and [10].

1. M is a good approximation to A in some sense

2. The cost of the construction of M is not prohibitive

3. The system $M^{-1}x = b$ is much easier to solve than the original system

We may choose appropriate precondition matrix M according to the criteria above. However, it is not necessary to solve the problem $M^{-1}Ax = M^{-1}b$; it only requires modifying the original CG algorithm into a preconditioned version. We will derive the PCG algorithm based on the CG Algorithm introduced in Section 3.3. Some parts of this derivation can be found in [14].

Assuming M is a symmetric positive-definite matrix, the Cholesky factorization of M is S. That is $M = SS^T$. The matrix $M^{-1}A$ will have the same eigenvalues as $S^{-1}AS$. The system $Ax = b$ can be transformed to $S^{-1}AS^{-T}\hat{x} = S^{-1}b$, $x' = S^Tx$. Then the matrix $S^{-1}AS^{-T}$ is also a symmetric positive-definite matrix, so we can apply the CG method to solve the above question, as follows

$$r_0' = S^{-1}b - S^{-1}AS^{-T}x_0', \; g_0 = r_0$$

for j=0~convergence

$$\alpha_j = r_j'^T r_j' \Big/ g_j'^T S^{-1}AS^{-T} g_j',$$

$$x_{j+1}' = x_j' + \alpha_j g_j'$$

$$r'_{j+1} = r'_j - \alpha_j S^{-1} A S^{-T} g'_j$$

$$\beta_j = r'^T_{j+1} r'_{j+1} \big/ r'^T_j r'_j$$

$$g'_{j+1} = r'_{j+1} + \beta_j g'_j$$

Then we define $r'_j = S^{-1} r$, $g'_j = S^T g_j$, above algorithm can be rewritten as

$$r_0 = b - Ax_0, \; g_0 = r_0$$

for j=0~convergence

$$\alpha_j = r^T_j M^{-1} r_j \big/ g^T_j A g_j$$

$$x_{j+1} = x_j + \alpha_j g_j$$

$$r_{j+1} = r_j - \alpha_j A g_j$$

$$\beta_j = r^T_{j+1} r_{j+1} \big/ r^T_j r_j$$

$$g_{j+1} = r_{j+1} + \beta_j g_j$$

End

Then we define $z_j = M^{-1} r_j$, and substitute above algorithm. We can derive the PCG algorithm [9], [15].

Algorithm 4.1 Preconditioned Conjugate Gradient Method

$r_0 = b - Ax_0, \ g_0 = r_0$

for j=0~convergence

$\mathrm{z}_j = M^{-1} r_j$

$\alpha_j = r_j^T z_j \big/ g_j^T A g_j$

$x_{j+1} = x_j + \alpha_j g_j$

$r_{j+1} = r_j - \alpha_j A g_j$

$\beta_j = r_{j+1}^T z_{j+1} \big/ r_j^T z_j, \ \ g_{j+1} = z_{j+1} + \beta_j g_j$

4.3.2 PCG LMMSE Equalizer

The LMMSE equalizer for mobile OFDM system has introduced in Section 4.2, the weights is calculate by Equation (4.3). The equalized signal can be written as

$$\mathbf{d} = \mathbf{W}_{mmse}^H \mathbf{y} = \mathbf{A}^H (\mathbf{A}\mathbf{A}^H + \frac{1}{\mathbf{SNR}} \mathbf{R}_{zz})^{-1} \mathbf{y} \tag{4.10}$$

This equation above can be rewritten as

$$(\mathbf{A}\mathbf{A}^H + \frac{1}{\mathbf{SNR}} \mathbf{R}_{zz})\mathbf{e} = \mathbf{y} \tag{4.11}$$

$$\mathbf{d} = \mathbf{A}^H \mathbf{e} \tag{4.12}$$

By defining $\mathbf{T} = (\mathbf{A}\mathbf{A}^H + \frac{1}{\mathrm{SNR}} \mathbf{R}_{zz})$, Equation (4.9) is equivalent to solve a $\mathbf{T}\mathbf{d} = \mathbf{y}$ problem. Observing the equation above, an $N \times N$ matrix inversion is required. By the band channel approximation as described in Section 4.1, this matrix is a spare

symmetric positive definite matrix. The CG algorithm introduced in Chapter 3 is one of the best known iterative techniques for solving symmetric positive definite problem, but it may suffer the problem of low convergence rate. The PCG algorithm can be used to avoid this problem.

By observing the amplitude of the matrix $\mathbf{A}$ which is shown in Figure 4.1, it can be found that the most significant coefficients are those on the central band and the edges of the matrix. Then the matrix $(\mathbf{A}\mathbf{A}^H + \frac{1}{\mathbf{SNR}}\mathbf{R}_{zz})$ which is the matrix required to inverted still have similar characteristic to the matrix $\mathbf{A}$. It means that it is also a diagonal dominant system. By applying the three criteria described in the previous section, we can choose some diagonals of the central band of the matrix $(\mathbf{A}\mathbf{A}^H + \frac{1}{\mathbf{SNR}}\mathbf{R}_{zz})$ as the precondition matrix, M which is shown in Figure 4.5. The three preconditioning criteria described in the previous section should be checked before preconditioning. First, because the matrix has the most significant values on its diagonals, this choice of the precondition matrix is similar to the original matrix A. Second, we can obtain the precondition matrix directly from the matrix A, so there is no extra cost in constructing the precondition matrix. Third, the system $M^{-1}x = b$ can be easily solved by the band LDL^H factorization [7], [15] and the forward and backward substitutions which have lower complexity than the inversion of a general matrix.

With the precondition matrix chosen above, Equation (4.9) can be solved iteratively by the PCG method described in Section 4.2. The condition number of the original system and the preconditioned system are shown in Figures 4.5-4.6. It can be shown that the preconditioned system has much smaller condition number than the original system, so the preconditioned system will converge faster than the original system. The convergence rate and complexity analysis of this method are shown in Section 4.4 and Section 4.5. By these analyses, it is presented that this approach has

lower complexity than the method introduced in Section 4.2 but still have similar BER performance to that method.
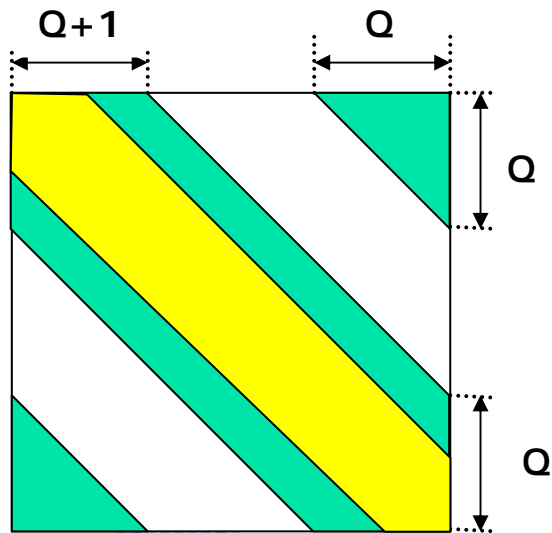

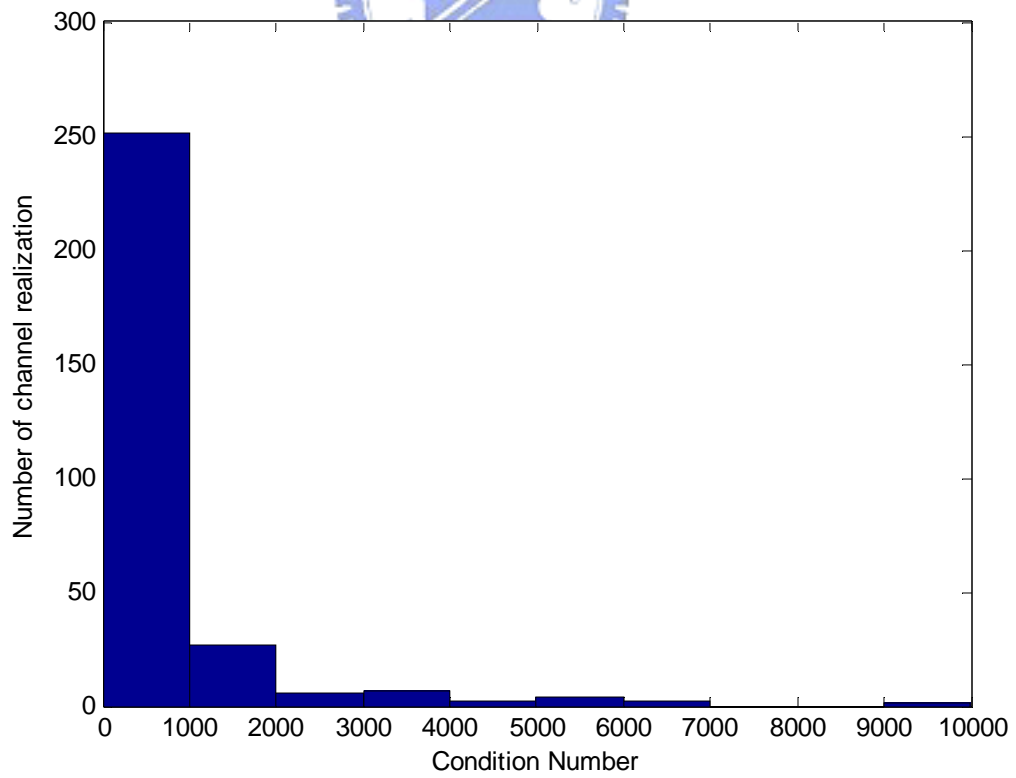. **Figure 4.5**: Structure of precondition matrix

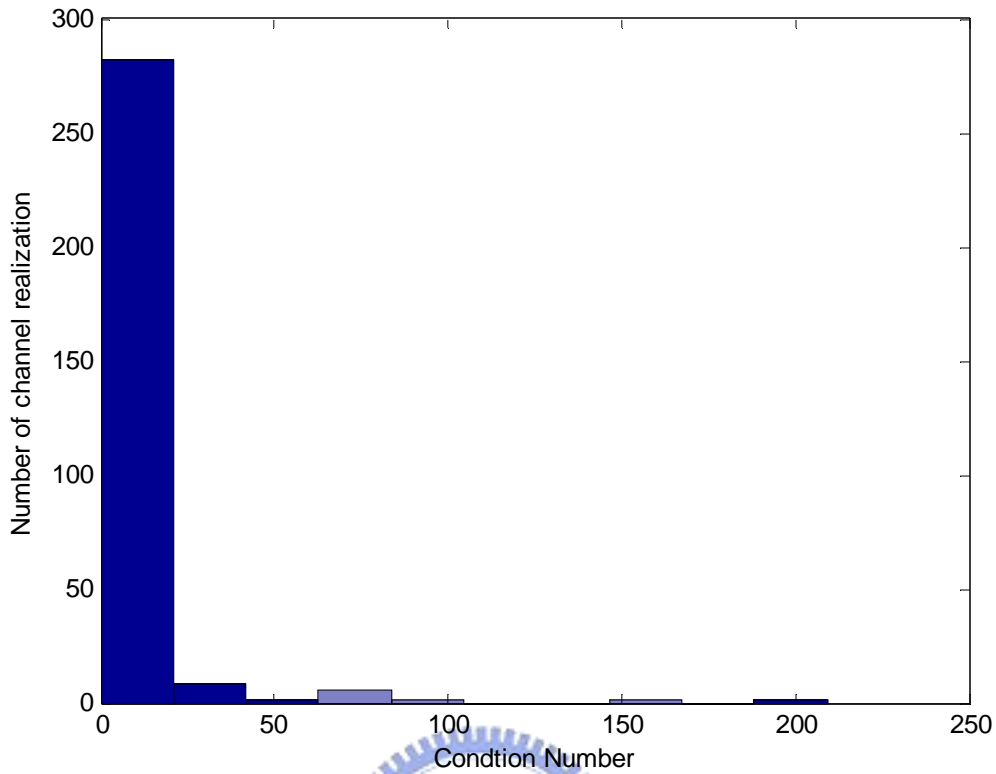**Figure 4.6**: Condition number of original system

Figure 4.7: Condition number of preconditioned system

4.3.3 Optimum Precondition Matrix

The central band of the matrix $(\mathbf{A}\mathbf{A}^H + \frac{1}{SNR}\mathbf{R}_{zz})$ is chosen as the precondition matrix in the previous section. Because we must solve the problem $M^{-1}x = b$ per iteration in Algorithm 4.1, it leads to some overhead problems. Because the complexity of the inversing a band system increases exponentially with the bandwidth of the matrix, it is a trade-off problem that how many bandwidth we should choose. Choosing a larger bandwidth of precondition matrix will let the system converge faster but it requires more computations per iteration, so the subset of the central band matrix may be chosen as the precondition matrix. By computer simulations and complexity analysis, we can obtain the optimum bandwidth of the precondition matrix that achieving the lowest complexity. We will discuss this in following section.

4.4 Complexity Analysis

The LMMSE proposed by Xiaodong Cai and Georgios B. Giannakis requires $O(N^2)$ flops, and the LMMSE method proposed by Philip Schniter which is called the Partial LMMSE method requires $O(N)$ flops. The PCG LMMSE method proposed by this paper also requires computations linearly with *N*. The complexity of the two methods, Partial LMMSE and PCG LMMSE will be analyzed here, and their complexity increases linearly with *N*.

A flop here is defined as a complex multiplication, and *N* is the FFT size, *P* is the bandwidth of the precondition matrix. Table 4.1 shows the complexity of PCG MMSE equalizer, and Table 4.2 shows the complexity of Partial MMSE equalizer

Note that the bandwidth of the precondition matrix not only affects the complexity per iteration but also the convergence rate. It is a trade-off that how many bandwidth of the original matrix required to choose for achieving the lowest complexity. The optimum bandwidth of the precondition matrix can be obtained by simulations. We will discuss the actual computation required by these two methods, Partial MMSE and PCG MMSE, in the next section.

Table 4.1: Complexity analysis of PCG MMSE equalizer

Operation	Complexity
$(\mathbf{AA}')$	$\left(2Q^2+Q+1\right)N$ flops
$\text{inv}(\mathbf{AA}'+\delta\mathbf{C}_{xx})*\mathbf{r}$	$\left(4Q+6+\dfrac{P^2}{2}+4P\right)\times\left(\text{number of iteration}\right)N$ flops
$\mathbf{H}'*inv(\mathbf{AA}'+\delta\mathbf{C}_{xx})*\mathbf{r}$	$\left(2Q+1\right)N$ flops
Total $\left\{\left(4Q+6+\dfrac{P^2}{2}+4P\right)\times\left(\text{number of iteration}\right)+2Q^2+4Q+2\right\}N$ flops	

Q : The bandwidth of the approximation channel

P : The bandwidth of the precondition matrix

N : FFT size

Table 4.2: Complexity analysis of Partial MMSE equalizer

Operation	Complexity
$\mathbf{R}_{Ai} = (\mathbf{A}_i \mathbf{A}_i\,')$	$\left(2Q^2 + 3Q + 1\right) N$ flops
$\text{inv}(\mathbf{AA}' + \delta \mathbf{C}_{xx}) * \mathbf{r}$	$\left(\dfrac{(2Q+1)^3}{6} + (2Q+1)^2\right) N$ flops
$\mathbf{h}' * \text{inv}(\mathbf{HH}' + \delta \mathbf{C}_{xx}) * \mathbf{r}$	$(2Q+1) N$ flops

Total $\left(\dfrac{4Q^3}{3} + 8Q^2 + 10Q + 3\right) N$ flops

Q : The bandwidth of the approximation channel

N : FFT size

4.5 Computer Simulations

In this section, computer simulations are conducted to evaluate the performance of the OFDM system using PCG LMMSE equalizer. Through out the simulations, we only deal with discrete time signal processing in the baseband, hence pulse-shaping and matched-filtering are removed from consideration for simplicity. Also, channel estimation and timing synchronization are assumed to be perfect. In the simulations, the relationship between SNR and E_b/N_0 is defined as

$$\frac{E_b}{N_0} = \frac{\text{bit power}}{\text{noise power}} = \frac{\frac{E_b}{T_s}}{N_0 B} = \frac{\frac{E_s}{T_s M}}{N_0 B} = \text{SNR} \cdot \frac{1}{M} \tag{4.13}$$

where E_s is the symbol energy, T_s is the symbol duration, B is the system bandwidth, and M is the modulation order. The system transmit bit power is normalized to one, the noise power given by σ^2 corresponding to a specific E_b/N_0 can be generated by

$$\sigma^2 = \frac{N_0}{E_b} \tag{4.14}$$

Table 4.3 lists all parameters used in our simulations. The configuration we consider here is an OFDM system with a bandwidth of 1.5 MHz and 64 subcarriers. The set of QAM constellation used in the simulations is QPSK. The channel model is the Jakes model [12], [17], [18] and the normalized Doppler spread equals 0.1.

Table 4.3: Parameters of Computer Simulations

Transmit/Receive antennas	SISO
Carrier frequency	5.2 GHz
Bandwidth	1 MHz
Number of carriers, FFT size	64
OFDM symbol duration	$42\,\mu$s
Guard interval	$5.25\,\mu$s
Modulation order	QPSK
Velocity	250 km/hour
Maximum Doppler frequency	1.2 KHz
Normalized Doppler frequency	0.05
Channel model	Jakes Model [17], [18]
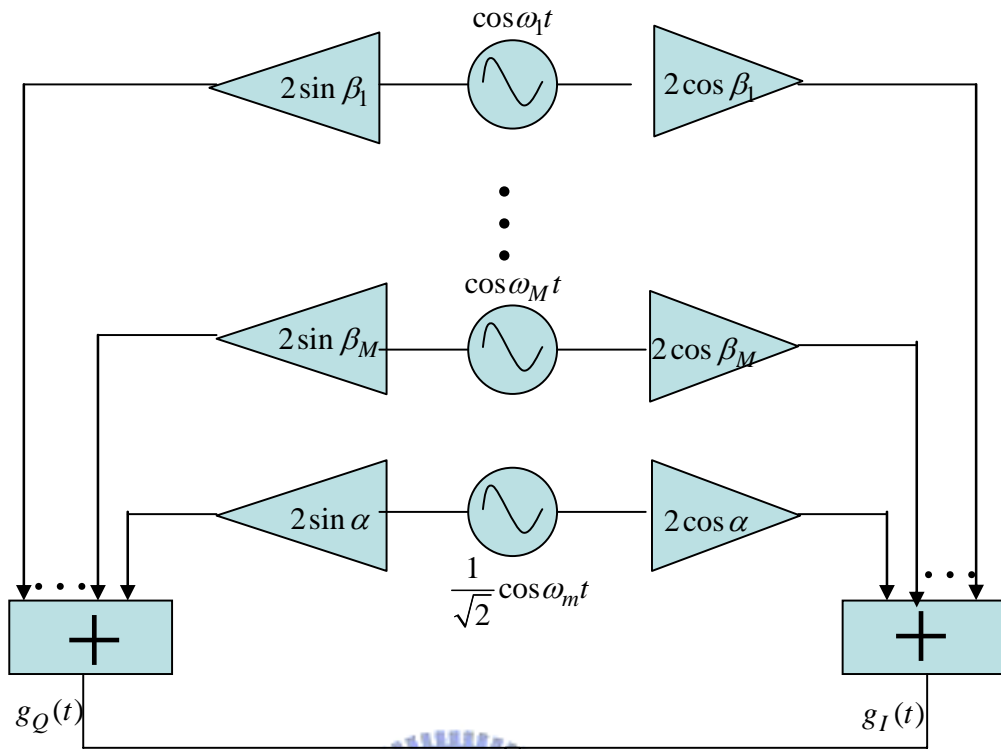
Figure 4.8: Jakes model simulator

The BER performances of the CG MMSE equalizer with different numbers of iterations are shown in Figure 4.10. It can be shown that the conventional CG algorithm suffers from slow convergence rate problem, and this problem can be solved by the PCG algorithm. The convergence rate of the proposed equalizer with different precondition matrix bandwidths is shown in Figures 4.11-4.14. It is shown that the convergence rate is proportional to the bandwidth of the precondition matrix, but a lager bandwidth of precondition matrix results in more computations per iteration. It is thus a trade-off in choosing the bandwidth of the precondition matrix. We define the complexity to be the number of multiplications per iteration multiplied by the number of iterations. In Table 4.2, we show the complexity of different bandwidths of the precondition matrix and the number of iterations required for the convergence. By the simulations result, we can determine the optimum bandwidth of the precondition

matrix. The optimum bandwidth of the precondition matrix here equals three. By the complexity analysis above, the PCG MMSE only requires 30% the computations of the Partial MMSE.
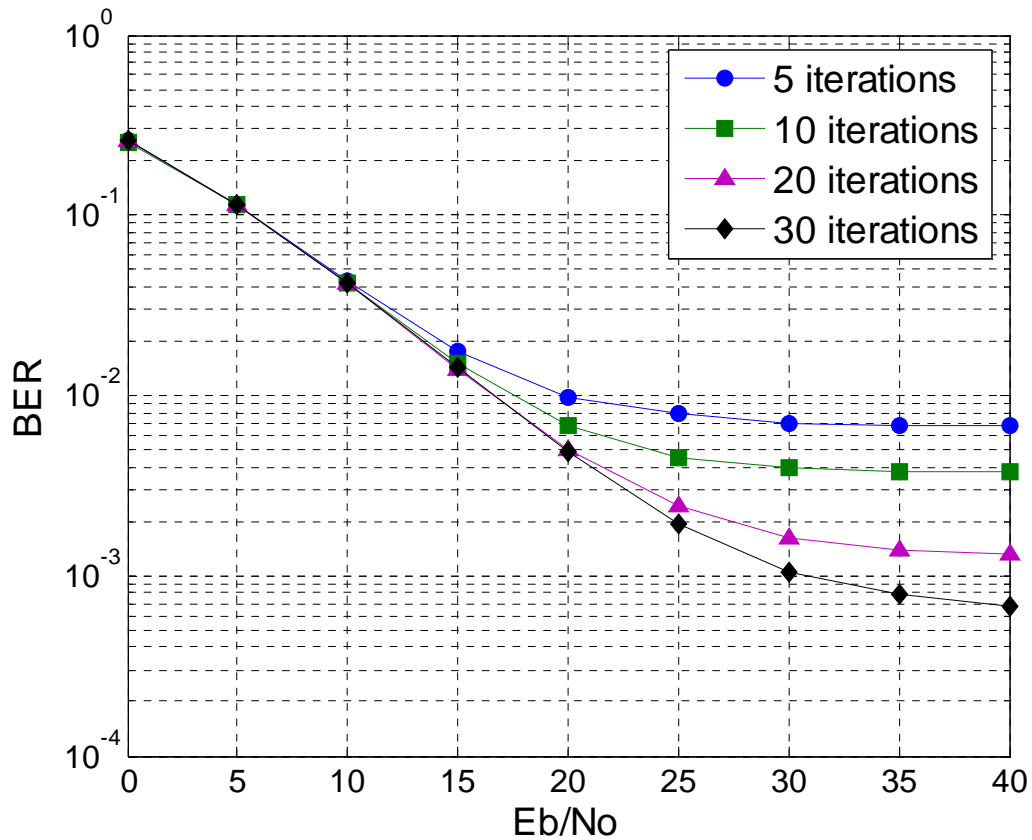

Figure 4.9: BER performance obtained by using CG based MMSE equalizer. The performance of different numbers of iterations is shown. It can be seen that it requires about 30 iterations to converge.
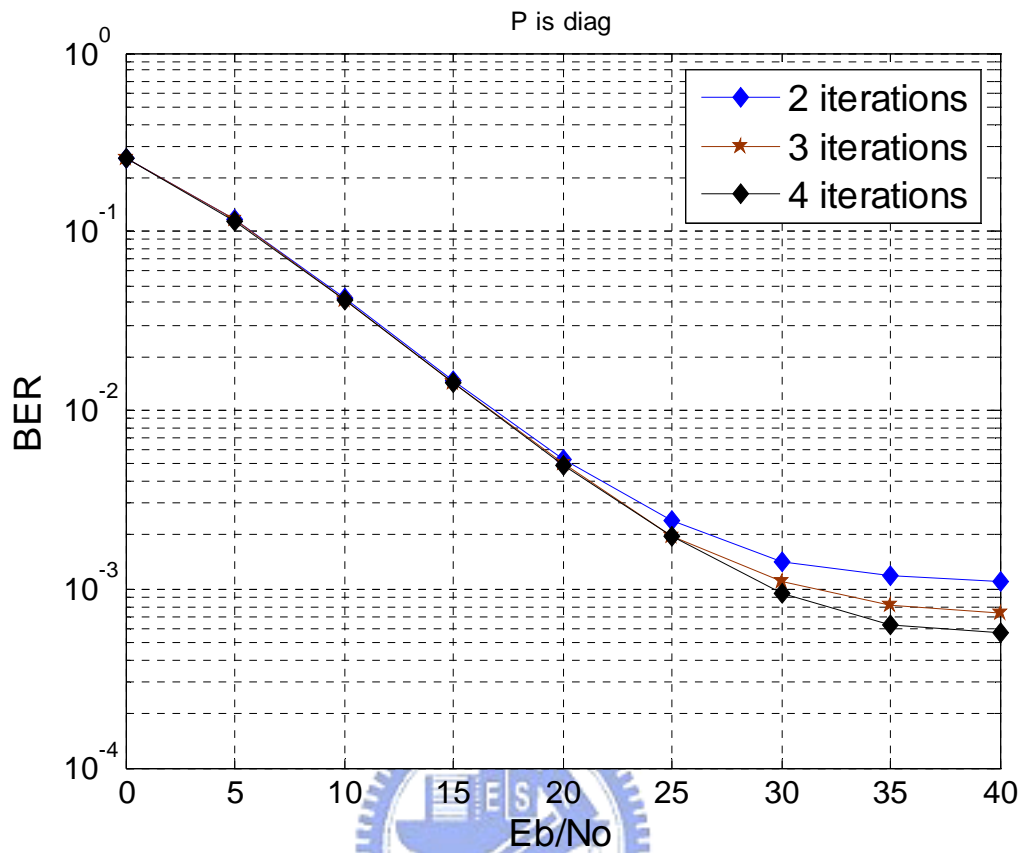
Figure 4.10: BER performance obtained by using PCG based MMSE equalizer, (BW of precondition matrix in PCG MMSE is zero). The performance of different numbers of iterations is shown. It can be seen that it requires about 4 iterations to converge.

Figure 4.11: BER performance obtained by using PCG based MMSE equalizer, (BW of precondition matrix in PCG MMSE is one). The performance of different numbers of iterations is shown. It can be seen that it requires about 3 iterations to converge.

Figure 4.12: BER performance obtained by using PCG based MMSE equalizer, (BW of precondition matrix in PCG MMSE is two). The performance of different numbers of iterations is shown. It can be seen that it requires about 2 iterations to converge.
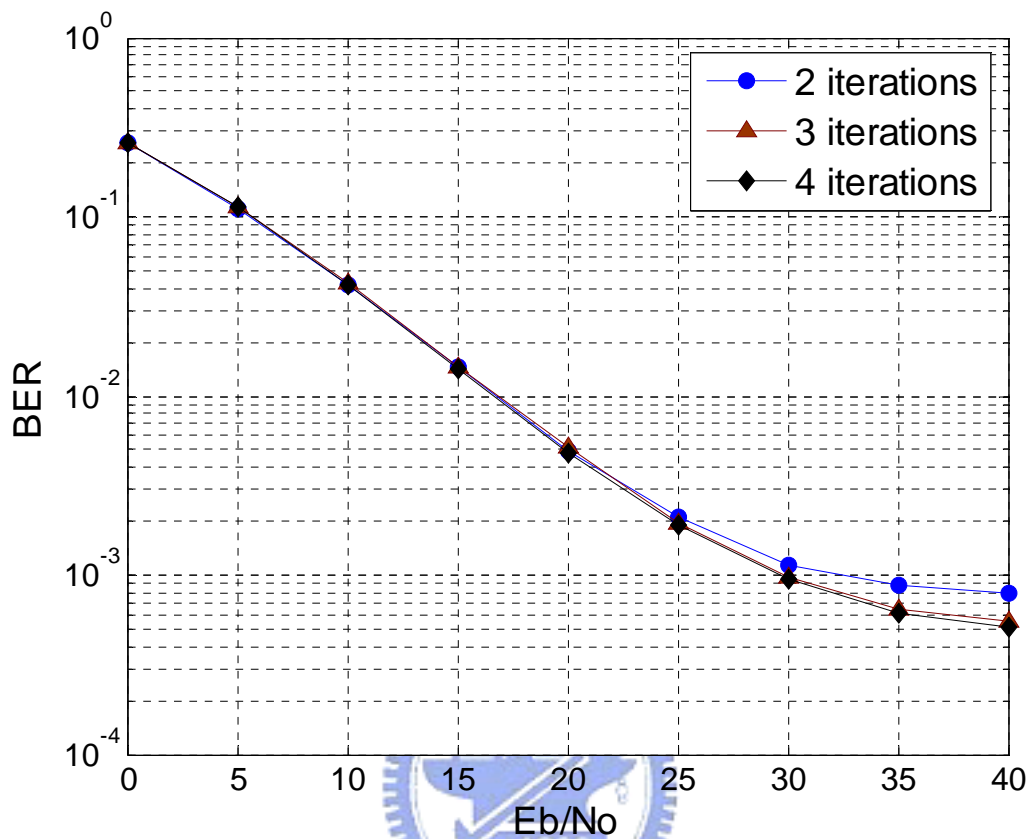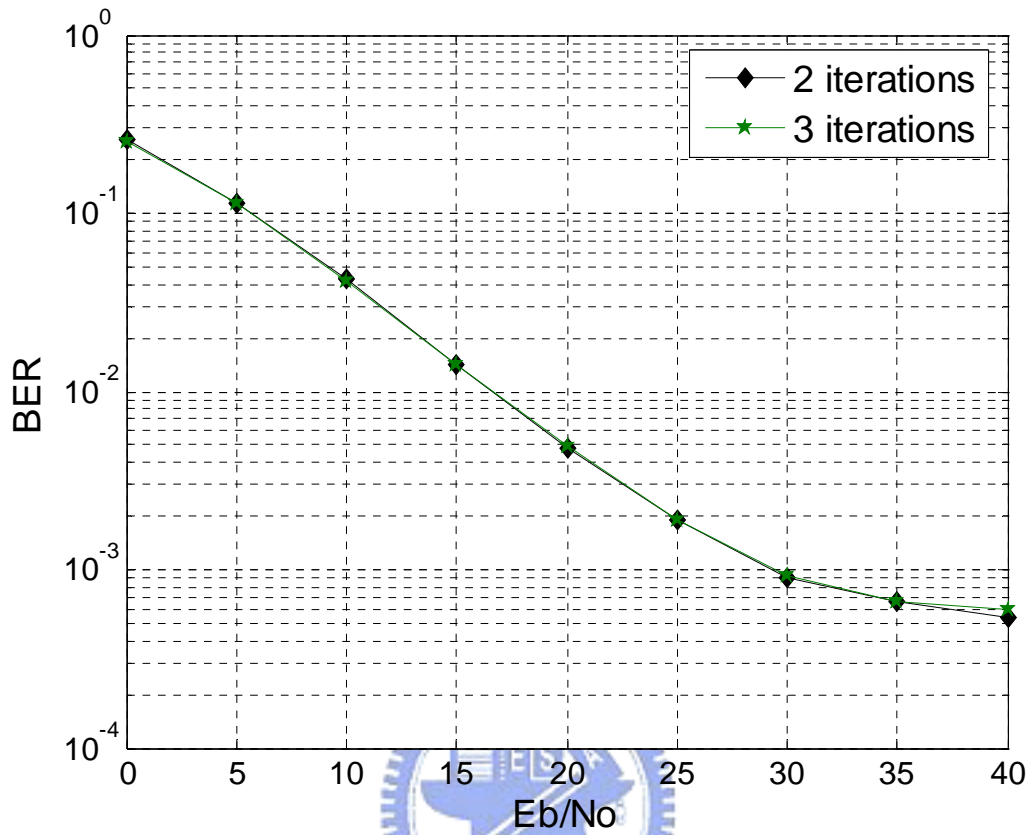
Table 4.4: Convergence rate for different precondition bandwidths

Precondition Matrix Bandwidth	Complexity $(4Q+6+1/2P2+4P)N$	Number of iterations
P=0	$(4Q+6)N$	4
P=1	$(4Q+10)N$	3
P=2	$(4Q+16)N$	2
P=3	$(4Q+22)N$	2

Figure 4.13 shows the BER performance of different schemes. The conventional one-tap equalizer scheme has poor performance due to the influence of ICI. The Partial MMSE and PCG MMSE have similar performance. A BER bound of the MMSE equalizer is also shown in this figure. The gap between the MMSE BER bound and the PCG MMSE is due to the channel approximation errors. This gap can be reduced by applying a more complicated method such as MMSE-SIC, MMSE-PIC [3], [4]. It shows that with the channel approximation the MMSE-PIC equalizer has better performance than the MMSE equalizer. The MMSE-PIC equalizer can even have better BER performance than the MMSE equalizer BER bound in low SNR region.
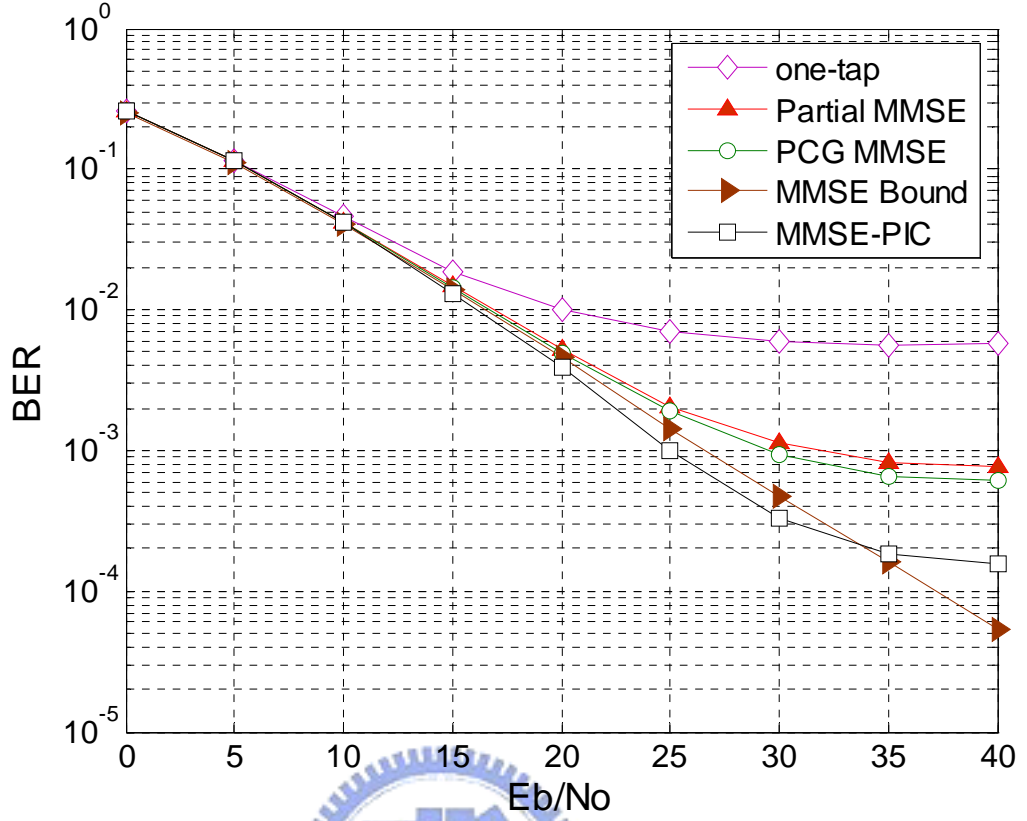
Figure 4.13: BER performance of different schemes

Figure 4.14 shows the BER performances under different vehicle speeds. The BER performance of the OFDM system degrades with an increasing vehicle speed because the ICI is more significant in the high mobility environments. It will thus require more bandwidth of the approximated channel or a complicated method to mitigate the ICI.

Figure 4.15 shows the BER performance with channel estimation errors. The channel estimation errors are defined as a AWGN noise with variance σ_e^2 to disturb the estimated channel taps, by the definition in [26]

$$\hat{\mathbf{h}}_t = \mathbf{h}_t + \mathbf{e} \tag{4.}$$

where $\hat{\mathbf{h}}_t = [\hat{h}(t,0), \hat{h}(t,1), \cdots \hat{h}(t,L-1)]$ is the estimated channel impulse response, and

$\mathbf{e}=\begin{bmatrix} e_1, e_2 \cdots e_{L-1} \end{bmatrix}$ represents the error vector. It is assumed that $\mathbf{e}$ is independent of $\mathbf{h}$ and is modeled as independent zeros means complex-valued Gaussian noise. It can be shown in Figure 4.18 that the PCG MMSE has similar performance to the Partial MMSE equalizer even if the channel estimation errors are considered. Because the Partial MMSE equalizer only takes parts of the equations, it may be more sensitive to the disturbance of channel.
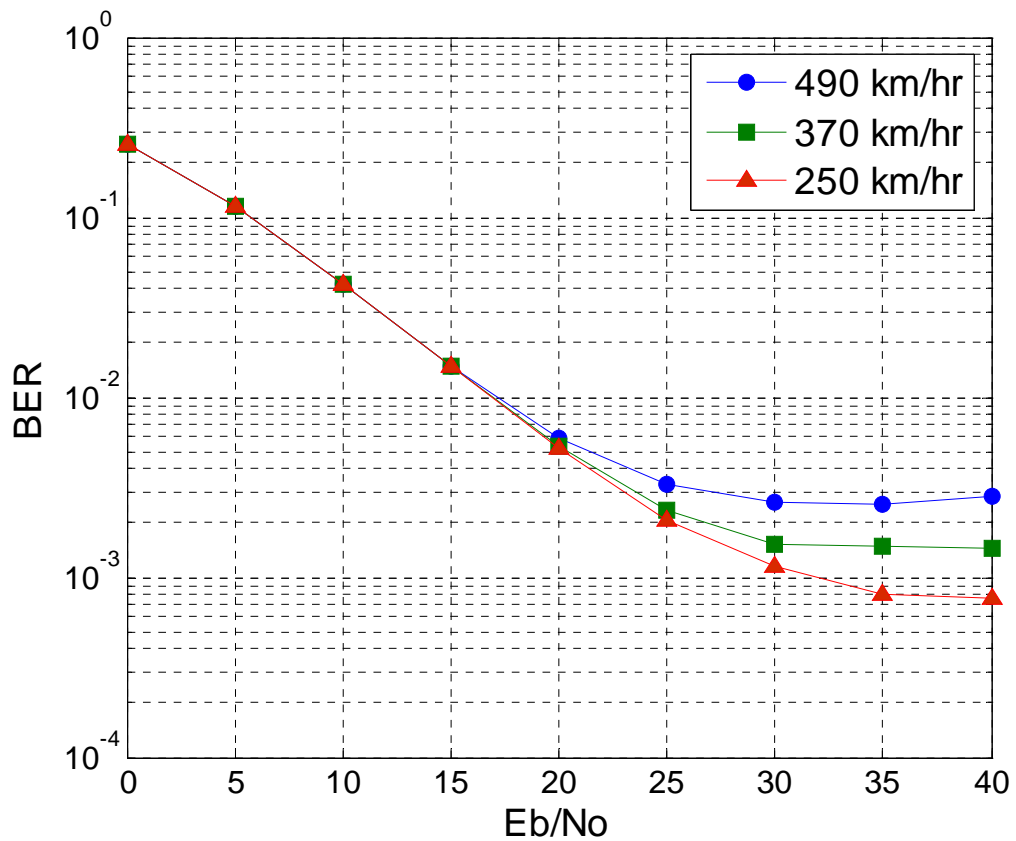

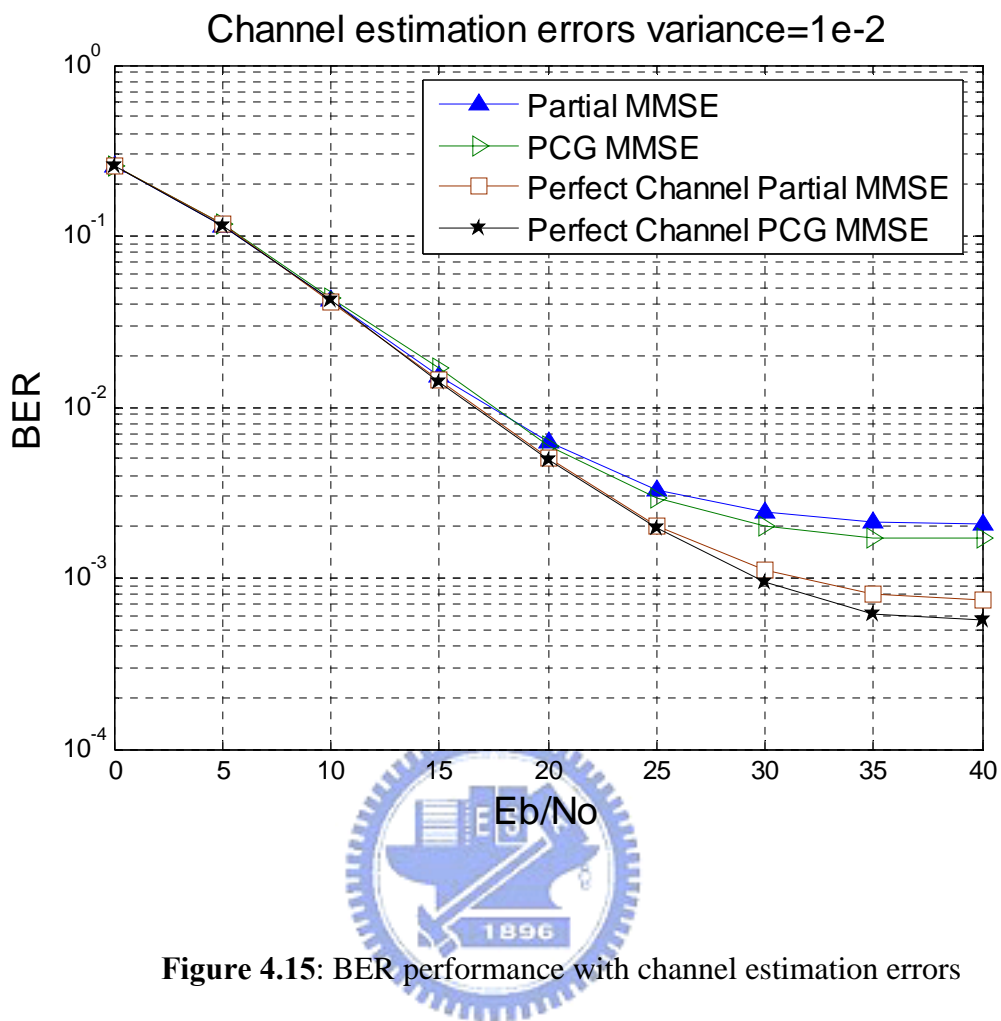**Figure 4.14**: BER performance under different vehicle speeds.

Figure 4.15: BER performance with channel estimation errors

4.7 Summary

In this chapter, we first introduce the channel approximation of mobile channel. This approximation is based on the concept that we are only concerned with the significant channel coefficients and ignore the trivial parts. With this approximation, the number of coefficients to be processed is reduced, so the computations for the equalizers can also be reduced. Although this approximation is useful, there is still an error floor due to the approximation errors. Furthermore, we introduce and compare several different low-complexity equalizers in Section 4.2, which are important techniques in this subject. By complexity analysis, it is shown that our scheme can achieve lower computation complexity while still have similar BER performance to the Partial MMSE equalizer.

.

Chapter 5

Conclusion

In this thesis, we propose a PCG based MMSE equalizer for the OFDM system over time-varying channels. Compared with conventional one-tap equalizers, this scheme can achieve better performance in mobile environments. In Chapter 2, the concept of OFDM system is introduced and the reason why OFDM system can be used efficiency in time-invariant channel is given. Besides, the challenges to OFDM system in mobile environments are introduced and mathematically analyzed. The most important issue is that the channel variations with time destroy the orthogonality between subcarriers and produce the intercarrier interference (ICI). Then the characteristics of the ICI are analyzed and the mobile channel matrix is approximated to a band matrix based on this ICI analysis. Furthermore, some basic techniques to cancel the ICI are introduced in this chapter, such as ICI self-cancellation schemes and the frequency domain equalizer schemes, the latter being adopted in this thesis In Chapter 3, we first introduce the idea of orthogonal projection and then derive the conjugate gradient (CG) algorithm. In Chapter 4, several schemes based on the frequency domain equalizer techniques are introduced, which have already been

proposed to cancel the ICI with moderate complexity. The CG method in Chapter 3 is modified into a preconditioned version and a PCG based low-complexity MMSE equalizer for canceling the ICI is proposed. Furthermore, the effect of the precondition matrix on the proposed method with different bandwidths is discussed. Then we analyze the complexity of this scheme and compare this scheme with other schemes.

The conventional system adopting the preamble to estimate the channel will have poor performance because of the channel variation with time. Actually, in a mobile OFDM system, it is necessary to insert sufficient pilot symbols for channel estimation. We can estimate the channel at some time instance and use linear or non-linear interpolation to obtain the entire time-varying channel estimate. There are still some problems in the estimation of time-varying channels because of the inaccuratcy of the interpolation. Besides, the condition number of the system decreases as the number of receiver antennas increases. This suggests that the proposed scheme can be better applide to the mobile MIMO-OFDM system.

Bibliography

[1] Y. Zhao, S. G. Haggman, "Intercarrier interference self-cancellation scheme for OFDM mobile Communication Systems", *IEEE Trans. on Communications*, vol. 49, no.7, pp.1185 – 1191, July 2001

[2] J. Armstrong, "Analysis of new and existing methods of reducing intercarrier interference due to carrier frequency offset in OFDM," *IEEE Trans. on COMMUNICATIONS*, vol.47, Issue 3, pp.365 – 369, March 1999

[3] X. Cai, G. B. Giannakis, "Bounding performance and suppressing intercarrier interference in wireless mobile OFDM", *IEEE Trans. on Communications*, vol. 51, no.12, pp.2047 – 2056, December 2003

[4] W. S. Hou, B. S. Chen, "ICI cancellation for OFDM communication systems in time-varying multipath fading channels", *IEEE Trans. on Wireless Communications*, vol. 4, no.5, pp.2100 – 2110, September 2005

[5] W. G. Jeon, K. H. Chang, Y. S. Cho, "An equalization technique for orthogonal frequency-division multiplexing systems in time-variant multipath channels", *IEEE Trans. on Communication*, vol47, pp.27~32, Jan. 1999

[6] P. Schniter, **"Low-complexity equalization of OFDM in doubly selective channels"**, *IEEE Trans. on Signal Processing*, vol.52, Issue 4, pp.1002~1011, April 2004

[7] L. Rugini, P. Banelli, G. Leus, "Simple equalization of time-varying channels for OFDM", *IEEE Communication Letters,* vol.9, Issuse 7, pp.619~621 July 2005

[8] O. Axelsson, *Iterative Solution Methods*, Cambridge University Press, 1994

[9] Y. Saad, Iterative Methods for Sparse Linear Systems, 2nd ed. SIAM, 2003

[10] H. A. van der Vorst, *Iterative Krylov Methods for Large Linear Systems*, Cambridge University Press, 2003

[11] B, Richard, Templates for the solution of linear systems/Building blocks for iterative methods SIAM, 1994

[12] W. C. Jakes, *Microwave mobile communications,* John Wiley & Sons, Inc., 1974

[13] A. Seyedi, "General ICI self-cancellation scheme for OFDM systems", *IEEE Trans. on Vehicular Technology,* vol. 54, no.1, pp.198 – 210, January 2005

[14] J. R. Shewchuk, "An introduction to the conjugate gradient method without the agonizing pain", [Online], August 1994

Available: http://www.cs.cmu.edu/painless-conjugate-gradient.pdf

[15] G. H. Golub and C. F. Van Loan, *Matrix Computations*, 3rd ed. Johns Hopkins Univ. Press, 1996

[17] G. L. Stuber, *Principles of mobile communication*, 2nd ed. Kluwer Academic Publishers, 2001

[18] Y. R. Zheng, C. Xiao, "Improved models for generation of multiple uncorrelated Rayleigh fading waveforms", *IEEE Communications Letters,* vol. 6, no.6, pp.256 – 258, June 2002

[19] J. Li, M. Kavehrad, "Effects of time selective multipath fading on OFDM systems for broadband mobile applications", *IEEE Communications Letters,* vol. 3, no.12, pp.332 – 334, December 1999

[20] P. Robertson, S. Kaiser, "The effects of Doppler spreads in OFDM(A) mobile radio system", *IEEE Vehicular Technology Conference*, vol.1, pp.329~333, September, 1999

[21] I. Barhumi, G. Leus, M. Moonen, "Time-varying FIR equalization for doubly selective channels", *IEEE Trans. on Wireless Communications*, vol. 4, Issue 1, pp.202 – 214, Jan. 2005

[22] A. Stamoulis, S. N. Diggavi, N. Al-Dhahir, "Intercarrier interference in MIMO OFDM", *IEEE Trans. on Signal Processing*, vol. 50, no.10, pp.2451 – 2463, October 2002

[23] L. Rugini, P. Banelli, G. Leus, "Block DFE and windowing for Doppler-affected OFDM systems", *IEEE 6th Workshop on Signal Processing Advances in Wireless Communications*, pp.470 – 474, 2005

[24] K. W. Park, Y. S. Cho, "An MIMO-OFDM technique for high-speed mobile channels", *IEEE Communications Letters,* vol. 9, no.7, pp.604 – 606, July 2005

[25] L. Yang, C. Ming, S. Cheng, "Intercarrier interference cancellation of OFDM for time-varying channels", *IEEE Communications Society Globecom,* 2004

[26] S. Takaoka; H. Gacanin, F. Adachi, "Impact of imperfect channel estimation on OFDM/TDM performance", *IEEE Vehicular Technology Conference*, vol.1, June 2005

[27] Y.-S. Choi, P. J. Voltz, and F. A. Cassara, "On channel estimation and detection of multicarrier signals in fast and selective Rayleigh fading channels", *IEEE Trans. on Communications*, vol. 49, pp.1375 – 1387, August 2001

[28] B. Stantchev and G. Fettweis, "Time-variant distortions in OFDM", *IEEE Communication Letters,* vol.4, pp.401–404, Mar 2001

[29] *Air interface for fixed and mobile broadband wireless access systems* (IEEE Std. 802.16e-2005 and IEEE Std 802.16-2004/Cor 1-2005), February, 2006

[30] L. Rugini, P. Banelli, G. Leus, "Low-complexity banded equalizers for OFDM systems in Doppler spread channels", *EURASIP Journal on Applied Signal Processing,* revised on Janunary 2006

[31] M. Guillaud, D. T. M. Slock, "Channel Modeling and associated inter-carrier interference equalization for OFDM systems with high Doppler spread", *ICASSP,* vol 4, pp. 237–240, April 2003

[32] S. Tomasin, A. Gorohov, H. Yang, J.P. Linnartz, "Iterative interference cancellation and channel estimation for mobile OFDM", *IEEE Trans. on Wireless Communications*, vol. 4, no.1, pp.238 – 245, January 2005

[33] B. Yang, Z. Cao, and K. B. Letaief, "Analysis of low complexity windowed DFT-based MMSE channel estimator for OFDM systems", *IEEE Trans. on Communications*, vol. 49, no.11, pp.1977 – 1987, November 2001